Endothelial progenitor cells as therapeutic tools in brain aging and disease

Ph.D. Dissertation

Lam Tri Duc

Supervisor: **Dr. Attila Elek Farkas**

Neurovascular Unit Research Group

HUN-REN Biological Research Centre

University of Szeged

Faculty of Science and Informatics

Doctoral School of Biology

2025

Table of Contents

LIST OF ABBREVIATIONS

EPC: Endothelial progenitor cell

MAgEC: Mouse aorta–gonad–mesonephros endothelial cells

BBB: Blood-brain barrier

EC: Endothelial cell

TJ: Tight junction

AD: Alzheimer's disease

PD: Parkinson's disease

ALS: Amyotrophic lateral sclerosis

HD: Huntington’s disease

FTD: Frontotemporal lobar dementia

IS: Ischemic stroke

SASP: Senescence-associated secretory phenotype

NVU: Neurovascular unit

abt-263: Navitoclax

Q+D: Quercetin + Dasatinib

VEGF: Vascular Endothelial Growth Factor

Aβ: Amyloid-beta

TDP-43: TAR DNA-binding protein 43

mAbs: Monoclonal antibodies

TTC: 2,3,5-triphenyltetrazolium chloride

TNFα: Tumor necrosis factor-alpha

PBS: Phosphate-buffered saline

PFA: Paraformaldehyde

BSA: Bovine serum albumin

CCA: Common carotid artery

CBF: Cerebral blood flow

LIST OF TABLES

LIST OF FIGURES

1. INTRODUCTION

Societies and economies of developed countries are encountering unprecedented challenges due to the rapidly expanding older population. In 2020, the number of individuals aged over 65 reached a staggering 727 million (*World Population Ageing 2020 Highlights*, 2020). Projections indicate that by the year 2050, this number will more than double, with seniors constituting up to 16% of the population, equating to one in every six individuals (*World Population Ageing 2020 Highlights*, 2020). Aging, while not a disease in itself, brings about a series of physiological changes that are largely inevitable and correlate with a surge in brain-related diseases such as Alzheimer's disease, amyotrophic lateral sclerosis (ALS), Parkinson's disease, strokes, and tumors (Azam et al., 2021).

At the tissue level, aging causes an increase in the number of senescent cells, which are incapable of proliferation and hinder the formation of new blood vessels and the repair of damaged endothelium. Endothelial senescence is linked with endothelial dysfunction, arterial stiffening, impaired angiogenesis, defective vascular repair, and an increased prevalence of atherosclerosis (Erusalimsky, 2009). At the microvascular level of the brain, aging is associated with increased capillary diameters, decreased capillary density, and heightened red blood cell velocities (Brown & Thore, 2011; Desjardins et al., 2014). Repairing brain vasculature should improve brain functions, thus we looked at ways to achieve this.

Since it was shown that reducing the number of senescent cells using senolytics can significantly increase the lifespan of mice there has been an increased interest in research studying the therapeutic use of senolytics (Xu et al., 2018). Studies have shown that senolysis in the aging brain via senolitics leads to improved blood-brain barrier (BBB) properties and reduced neuroinflammation (Yao et al., 2024). Our theory was that this treatment could be combined with endothelial progenitor cells (EPCs) therapy for a more significant effect. The positive effect of EPC therapy on neurogenesis after ischemic injury is well-documented (Esquiva et al., 2018). Still, the effect of EPCs under physiological conditions or in aging needs to be better studied.

Another field in which EPCs are promising is the delivery or in situ production of therapeutics in the brain (Cheng et al., 2023; Collet et al., 2016). As antibody therapies against misfolded proteins and their aggregates in the brain face difficulties in reaching their targets (Kouhi et al., 2021), we entered a collaboration to use EPCs as antibody factories against TDP43. In the following part of the introduction, I will detail the topics connected to this research.

2. LITERATURE BACKGROUND

2.1 Aging

Nowadays, the issue of aging is pressing, as it presents unresolved health and socioeconomic challenges. The aging process is inevitable, intricate, and heavily influenced by genetics and various environmental factors, including dietary choices, levels of physical activity, exposure to microbes, pollutants, ionizing radiation, and psychological factors (Plagg & Zerbe, 2020). Aging is a multi-level phenomenon impacting multiple organs at molecular and cellular levels (Katsagoni et al., 2023). Among the most notable manifestations of aging is the gradual decline in the functional capabilities of our brain. This decline encompasses various aspects, including memory, learning, motor coordination, decision-making speed, attention, and sensory perception such as taste, touch, vision, smell, and hearing (Alexander et al., 2012). As individuals age, changes occur in neurons' biological, chemical, and physical properties. Additionally, aging serves as a significant risk factor for various neurological diseases, including Alzheimer's disease (AD), Parkinson's disease (PD), amyotrophic lateral sclerosis (ALS), Huntington's disease (HD), and frontotemporal lobar dementia (FTD) and stroke (Azam et al., 2021; Kesidou et al., 2023; Navakkode & Kennedy, 2024). The cellular and molecular hallmarks of aging include accumulating oxidatively damaged proteins, nucleic acids, and lipids; dysfunctional neuronal calcium homeostasis; compromised DNA repair; exhaustion of stem cells; glia cell activation and inflammation; mitochondrial dysfunction; impaired molecular waste disposal; aberrant neuronal network activity; impaired adaptive stress response signaling; and dysregulated energy metabolism (Figure 1) (Mattson & Arumugam, 2018).

Neuron function depends on brain homeostasis, which is maintained by the neurovascular unit (NVU) that is comprised of neural and vascular cell types. The two main NVU functions responsible for brain homeostasis are the neurovascular coupling and the blood-brain barrier. It is becoming clear that glial cells – that support neurons both physically and chemically - play important roles in aging (Salas et al., 2020). Similarly, endothelial cells that are responsible for the blood-brain barrier - the strict control of nutrient and waste transport between the blood and the brain tissue - also develop dysfunction with aging (Carracedo et al., 2018). Increased blood-brain barrier permeability was observed in healthy individuals as early as the age of 40 (Montagne et al., 2015).

The complex biological network of the aging process is characterized by an increased number of senescent cells. While senescence aids tissue remodeling during development and following damage, it can also impair tissue regeneration, leading to inflammation and the emergence of numerous chronic illnesses or tumors (Muñoz-Espín & Serrano, 2014).

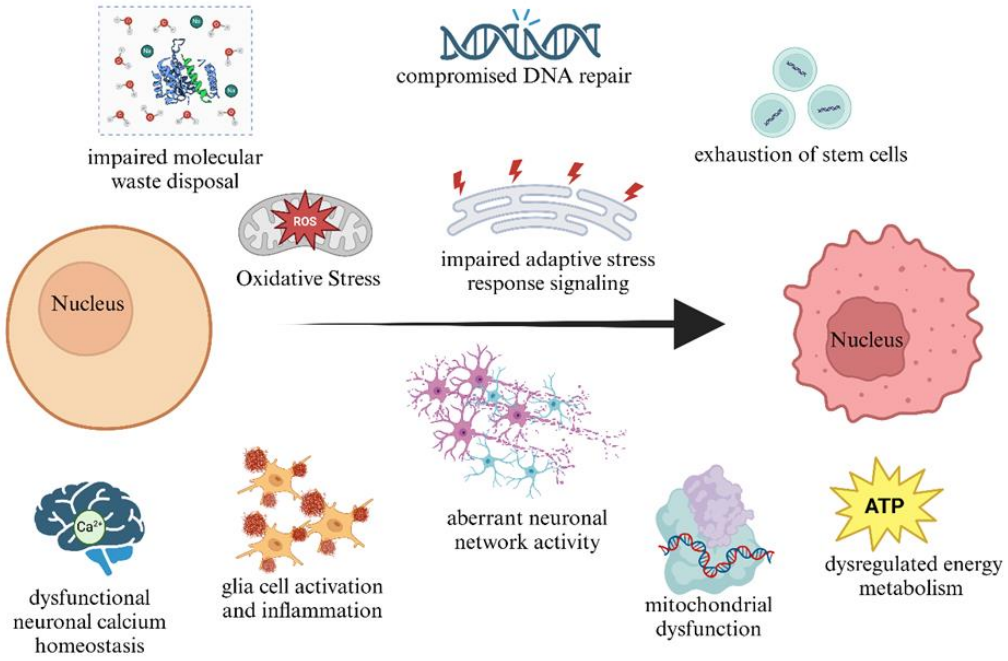

Figure 1. Hallmarks of aging

2.2 Senescence

Originally recognized as the limited replicative capacity of primary cells *in vitro*, senescence plays significant roles in living organisms as well (Kuilman et al., 2010). Senescent cells are arrested in replication, are resistant to apoptosis and undergo further phenotypic changes - the senescence-associated secretory phenotype (SASP) - that results in the secretion of high levels of inflammatory cytokines, chemokines, growth factors, and proteases.

On one hand senescence is a beneficial process as it plays roles in tissue remodeling during development or in response to injury and is an important anticancer process as it can prevent cells with damaged genomes from proliferating uncontrollably. The secretion of proinflammatory mediators can boost immune response and tissue repair. Cellular senescence can be triggered by several factors, including oncogene activation, irradiation, DNA damage, and telomere shortening. On the other hand, mutations in essential genes that induce cell cycle arrest via senescence may result in the immortalization of cells, increasing their lifespan and

raising the risk of cancer. Physiologically, the senescent cells are cleared by the immune system, but this process becomes less efficient during aging (Burton & Krizhanovsky, 2014). As the number of senescent cells increases, the secreted proinflammatory factors can limit tissue regeneration by impairing stem and progenitor cell function and also cause tissue damage that can promote age-related diseases and cancer.

2.3 Senolysis

Senescence is being recognized to be central in the aging process and many pathologies. Experimental introduction of senescent cells in mice decreased their lifespan (Xu et al., 2018). Senolysis, the removal of senescent cells was predicted to prolong the lifespan and health span.

Targeted removal of senescent cells was made possible first in a mouse model strain called INK-ATTAC. In these transgenic mice, senescent cells can be eliminated through the inducible activation of a modified caspase-8 gene in cells expressing a biomarker of senescence: p16(Ink4a). This was able to inhibit the appearance of senescence-associated tissue dysfunction and thus increase the health span (Baker et al., 2011). This tool proved to be invaluable and has since been used to uncover many details of how senescence is connected to aging and age-related pathologies (Melo Dos Santos et al., 2024). As the molecular mechanisms of senescence were becoming known, a new class of drugs, termed senolytics were introduced targeting the apoptosis resistance of senescent cells (Zhu et al., 2015).

Anti-apoptotic signaling was already well-studied in cancer research, thus the first senolytics were repurposed anticancer drugs (Kirkland & Tchkonia, 2020). Dasatinib (D) is an anticancer, broad-spectrum tyrosine kinase inhibitor drug targeting multiple tyrosine kinases (Montero et al., 2011). Quercetin (Q), a natural flavonol that gives apple peel its bitter taste and inhibits the mTOR and PI3K signaling pathways (Bruning, 2013), was found to be more efficient at reducing the viability of senescent human umbilical vein endothelial cells (HUVEC) than Dasatinib (Zhu et al., 2015). The combination of D and Q has been shown to alleviate symptoms of age-related conditions in mouse models and improve survival in older mice (Xu et al., 2018; Zhu et al., 2015). Additionally, the removal of senescent cells using D+Q has been shown to restore the reparative functions of human cardiomyocytes and endothelial cells *in vitro* (Sunderland et al., 2023).

Further research, aimed at Bcl-2 family inhibition, confirmed that abt-263 (navitoclax) that inhibits Bcl-xl, Bcl-2, and Bcl-w was senolytic but TW-37 that targets Bcl-xl, Bcl-2, and

Mcl-1 was not (Zhu et al., 2016). Abt-263 showed cell type specificity based on the expression patterns of Bcl-2 family proteins. *In vivo* abt-263 treatment depleted senescent cells and mitigated total body irradiation-induced premature aging of the hematopoietic system and rejuvenated senescent hematopoietic and muscle stem cells in healthy, aged mice (J. Chang et al., 2016). Abt-263 has been shown to target and eliminate senescent cells involved in the development of atherosclerosis (Childs et al., 2016).

The search for further senolytic substances continues to be successful in broadening the repertoire available for clearing senescent cells. Piperlongumine is a senolytic molecule isolated from plants in the Piper genus and studied for its anticancer effects through ROS-independent signaling (Wang et al., 2016). Another natural product with senolytic properties is fisetin, which is a flavonoid present in many fruits and vegetables with the highest concentration found in strawberries. Two specific inhibitors of Bcl-xl, A1331852, and A1155463, were also found to be senolytic, potentially allowing more cell type-specific senolysis with fewer side effects (Zhu et al., 2017). A recent addition to the group of senolytic drugs, zoledronic acid was used for close to 20 years to decrease the risk of fractures. It was found to decrease mortality of patients and expand the lifespan and health span of animals, thus recently it was tested and confirmed for senolytic effect in animal experiments (Samakkarnthai et al., 2023).

2.4 Senolysis in the brain

The use of senolytics not only reduced the cognitive dysfunction caused by aging in mice and rats (Krzystyniak et al., 2022) but also showed positive effects in various disease models including neurodegenerative diseases. Both clearing senescent cells in the INK-ATTAC model or using D+Q treatment in aged wild-type mice improved vasomotor function in atherosclerosis (Roos et al., 2016). The clearance of senescent cells in multiple transgenic mouse models of neurodegenerative diseases – using the INK-ATTAC transgenic model or pharmacologically by senolytic treatments with abt-263 or D+Q – ameliorated neurodegenerative symptoms and improved cognition (Bussian et al., 2018; Musi et al., 2018; P. Zhang et al., 2019). Senolysis was also found neuroprotective following hypoxia (Lu et al., 2023), and could rescue paclitaxel-induced microvascular senescence and attenuate chemotherapy-induced cognitive impairment (Ahire et al., 2023). There are multiple clinical trials of senolysis going on currently (Chaib et al., 2022). Two of these were phase I trials that finished recently, with one focusing on brain function. The two small pilot studies established

the safety, tolerability, and feasibility of D+Q treatment in Alzheimer's disease and in idiopathic pulmonary fibrosis with promising albeit preliminary results (Gonzales et al., 2023; Nambiar et al., 2023).

2.5 Endothelial cells of the central nervous system

Endothelial cells (ECs) of mesodermal origin constitute the primary cellular lining of blood vessels, lymphatic vessels, and the heart (Bautch & Caron, 2015). Brain endothelial cells are specialized endothelial cells that form the inner lining of blood vessels in the central nervous system. These cells form the cellular basis of the blood-brain barrier that strictly regulates the transport of molecules and ions between the brain and the blood. One of the most important aspects of brain endothelial cells is the continuous intercellular connection provided by tight junctions. Aging and age-related neurological disorders affect the subcellular localization and expression level of claudin 5, which is the main transmembrane protein of brain endothelial tight junctions (Costea et al., 2019).

Vascular structures develop and grow through two major processes involving endothelial cells. Vasculogenesis is the process by which mesodermal cells, known as angioblasts, assemble to form new endothelial tubes in the developing embryo. Conversely, angiogenesis refers to the sprouting of vasculature from pre-existing vessels. Vasculogenesis was described as the process of new vessel formation during embryonic development. However, a similar process has also been discovered to occur during adult life (Dudley & Griffioen, 2023).

2.6 Endothelial progenitor cells

In 1997 Asahara and colleagues isolated CD34+, angioblast-like cells from peripheral blood that they called putative progenitor endothelial cells. These cells could be cultured *in vitro* and were able to home into angiogenic sites, differentiated into endothelial cells, and contribute to new vessel formation which is consistent with vasculogenesis (Asahara et al., 1997). These were later named endothelial progenitor cells or EPCs and started a new wave of research into their potential therapeutic use for example as vectors for treating cancer by targeting neovascularization for relieving regional ischemia. The following year bone marrow-derived precursor endothelial cells were described to differentiate into endothelial cells *in vivo* in a dog model (Shi et al., 1998). These experiments and others presented evidence that EPCs in the circulation mobilize from the bone marrow in response to injury. This was later questioned as contradictory results were found while studying EPCs in samples from people

with sex-mismatched bone marrow transplantation (Fujisawa et al., 2019). Besides the debate about whether EPCs originate from bone marrow or from mature vasculature, there are further discussions regarding the definition and types of EPCs as well (Aquino et al., 2021; Medina et al., 2017). Regardless of these differences, EPCs can, without question, promote revascularization and regeneration of tissue after injury. Their efficacy in multiple pathologies such as sepsis or diabetes and in tissue regeneration after trauma, inflammation, or ischemia-reoxigenation induced injury has been demonstrated in many organs such as the kidney, lung, bone, heart, and in the brain as well (Chen et al., 2022). Regarding the therapeutic use of EPCs in the brain most data is focused on stroke models where EPCs injected into the circulation can improve neurogenesis, possibly through neovascularization and improved BBB properties (Esquiva et al., 2018; Geng et al., 2017; Huang et al., 2020).

During embryogenesis, the cardiovascular system develops from mesodermal cells. RNA analysis of isolated embryonic EPCs from 7.5 days post conception (dpc) murine embryos showed the expression of endothelial genes tie-2 and thrombomodulin but not that of VEGF receptors without the induction of endothelial differentiation (Hatzopoulos et al., 1998). The embryonic EPCs homed to areas of hypoxia, did not cause tumors and secreted many factors of angiogenesis, organogenesis, and tissue remodeling (Kupatt, Horstkotte, et al., 2005). Embryonic EPCs do not express major histocompatibility class I proteins, thus are not rejected by the host and avoid elimination by natural killer cells (Wei et al., 2004), as was demonstrated by Kupatt and colleagues after injecting murine embryonic EPCs into rabbits (Kupatt, Hinkel, et al., 2005) and pigs (Kupatt, Hinkel, et al., 2005) did not trigger an acute immune response but increased neovascularization and tissue regeneration. Embryonic EPCs in the aorta–gonad–mesonephros (AGM) of murine embryos diverge from hemangioblasts and become committed to the endothelial lineage at 10.5 dpc. EPCs isolated at this time point already express VEGF receptors, VE-cadherin and other endothelial markers, and the stem cell marker Sca-1 and the hematopoietic stem cell marker CD34. Immortalized AGM derived EPCs named MAgEC 10.5 (mouse AGM endothelial cells, 10.5 dpc) and MAgEC 11.5 (isolated at dpc 11.5) demonstrated angiogenic activity *in vitro*, homed in on hypoxic areas *in vivo* and cooperated with mature endothelial cells to form tube-like structures and penetrate tumor spheroids through a vasculogenesis-like process (Collet et al., 2016; Klimkiewicz et al., 2017).

2.7 EPCs in ischemic stroke

Hypoxia is a pathological condition characterized by insufficient oxygen delivery, either generalized or tissue hypoxia. In the brain – besides respiratory or heart emergencies – mainly hypoxic and in a smaller number hemorrhagic stroke causes tissue hypoxia. Stroke is a leading cause of mortality and disability. In aging populations – such as Europe – its incidence is expected to increase dramatically in the first half of the 21st century (Béjot et al., 2016; OECD & European Union, 2022).

Clinical studies showed that a higher number of circulating EPCs correlated with better outcomes of stroke. Furthermore, the serum levels of VEGF, angiopoietin 1, brain-derived neurotrophic factor and stromal cell-derived factor-1α correlated with CD34+ cell numbers in patients' blood samples. As these factors mobilized EPCs from the bone marrow in animal experiments it is likely that mobilization of EPCs from the bone marrow after stroke plays an important role in humans as well (Sobrino et al., 2011). In cerebral small vessel disease, the number of circulating CD34+CD133+CD309+ EPCs correlates with disease burden although it is not yet known whether the increased EPC number is beneficial in this case (Kapoor et al., 2021a).

Considering the promising results of animal experiments, there are very few clinical trials that finished with results (Custodia et al., 2022a). The trials all used different protocols for EPC isolation, thus EPCs of different origins and subtypes were collected and expanded *in vitro* before injection into the circulation of patients. Nevertheless, these trials showed that autologous EPC treatment was not just feasible and safe but also promising based on 6 months follow up in multiple treatment protocols: bone marrow-derived mononuclear cells injected after subacute ischemic stroke (Moniche et al., 2012), CD34+ selected peripheral blood-derived EPCs injected after acute ischemic stroke (Banerjee et al., 2014), CD34+ cells isolated after mobilization with granulocyte colony-stimulating factor and injected in aged ischemic stroke patients (Sung et al., 2018). Similarly, the only placebo-controlled, randomized trial with 4 years of follow-up found no adverse effect of the treatment and promising albeit not statistically significant functional benefits (Fang et al., 2019).

2.8 EPCs in neurodegenerative diseases

Neurodegenerative diseases are an increasing problem in aging populations and are more and more recognized to have neurovascular components. Multiple studies have examined

whether EPC numbers are affected by AD and other neurovascular pathologies. Although there were some contradictory results the consensus appeared to be that lower EPC count was associated with worse disease outcome (Rudnicka-Drożak et al., 2022). Currently, no clinical trials have investigated the use of EPCs in treating AD. However, there were preclinical studies on animal models. After EPCs injection into the hippocampal regions, APP/PS1 transgenic mice exhibited notable enhancements in spatial learning and memory abilities. Additionally, there was an increase in the expression of tight junction proteins (ZO-1, Claudin-5, and Occludin), a decrease in amyloid-beta (Aβ) plaque accumulation, and a reduction in hippocampal cell apoptosis (S. Zhang et al., 2018). A study showed that exogenous EPCs injected into Alzheimer's disease model APP/PS1 transgenic mice integrated into brain tissue at significantly higher levels than in wild-type mice, indicating that the pathological environment may promote EPC homing and integration (Yuan et al., 2016).

Accumulation of misfolded protein aggregates is characteristic of the progression of multiple neurodegenerative (Jo et al., 2020). For example, amyloid-β forms the pathological aggregates in AD (Tiwari et al., 2019), while α-synuclein defines PD pathology (Atik et al., 2016). In ALS, the accumulation of TAR DNA-binding protein 43 (TDP-43) aggregates is a key feature (Steinacker et al., 2019). TDP-43, encoded by the TARDBP gene, is a nuclear protein in the hnRNP family that can become cleaved, hyperphosphorylated, and ubiquitinated in disease states. ALS is a common motor neuron disorder, characterized by the degeneration of upper and lower motor neurons. As ALS progresses, p-TDP-43 lesions increase, leading to further motor neuron death (Braak et al., 2013). Monoclonal antibodies (mAbs) have been developed to clear misfolded proteins and their aggregates (Kwong et al., 2014). However, all phase-III clinical trials have been unsuccessful in hitting major endpoints because of the extremely efficient filter of BBB. Less than 1% of a small faction crosses the BBB (Zuchero et al., 2016). Successful delivery of therapeutic agents across the BBB requires structurally healthy blood vessels, normal vascularization, adequate blood flow, and recruitment of solute carrier-mediated transport or receptor-mediated transcytosis systems (Sweeney et al., 2019).

Thus, EPCs could be therapeutic tools to repair the damaged vasculature. EPC therapeutic effect could be further enhanced if EPCs were modified to express therapeutic antibodies locally in brain tissue.

3. OBJECTIVES

There is no clear consensus on how endothelial progenitor cells are able to improve neural function and repair and there is little known about their function in aging. The few studies that mention the localization of EPCs study tissue regeneration in response to ischemic injury. Consequently, there is a need for more detailed research to learn whether these cells adhere to the brain vasculature transiently or are able to integrate into it. Therefore, the goals of this thesis were:

• To study the dynamics of EPC-brain vasculature interactions under physiological conditions, in aging and in response to ischemic injury.

• To study a novel approach using *ex vivo* transfected EPCs as cellular producers of antibody fragments targeting misfolded proteins implicated in neurodegeneration.

• To study whether senolytic pre-treatment using abt-263 or the combination of dasatinib and quercetin can increase EPC interactions with the brain vasculature.

4. MATERIALS AND METHODS

4.1 Cell culture

MAgEC10.5 and tdTomato expressing MAgEC10.5 cells (C. Kieda Patents Nr 99-16169, WO-9631178B2) were described earlier (Collet et al., 2016; Thinard et al., 2022). In brief, the MAgEC10.5 cell line expressing tdTomato was generated using a third-generation lentiviral system, which included the plasmids pMDLg/pRRE, pRSV-Rev, and pMD2.G (gifted by Didier Trono, Addgene plasmid # 12251, 12253, 12259, Watertown, MA, USA) along with the expression vector pLV [3Exp]-EF1A>{tdTomato}:IRES: Puro (VectorBuilder, Chicago, IL, USA). Lentiviral vectors were produced using the Lenti-X™ 293T cell line (Clontech, Takara, Kusatsu, Japan), following the method described by Rossowska (Rossowska et al., 2017). After puromycin selection (10 µg/mL, Sigma-Aldrich, St. Louis, MO, USA), a stable MAgEC 10.5/tdTomato cell line was established and renamed MAgEC 10.5-tomato. Transduction efficiency and tdTomato fluorescence were analyzed using flow cytometry (FACS Aria, Becton Dickinson, Franklin Lakes, New Jersey, USA). Additionally, 4×10^5 MAgEC 10.5 cells labeled with CellTracker Red (C34552, Thermo Fisher, Waltham, MA, USA) were used, according to the manufacturer's instructions.

MAgEC10.5 cells were cultured in OPTIMEM I supplemented with 2% FBS (Thermo Fisher Scientific, Gibco, Waltham, Massachusetts USA) in a 5% CO_2 incubator at 37°C. Media was changed every 2-3 days, depending on cell numbers. Cultures were split at or before reaching confluence. For intracarotid injections, cells were seeded at a low density (500 000 cells per 3.5 cm diameter culture dish) the day before to ensure that cells were not clumped after trypsinization. Trypsin was used at 0.05% for passage and cell collection for 3 minutes. After stopping trypsin, a small volume was used to count cells in a hemocytometer. The rest was centrifuged for 5 minutes at 4°C at 700 RCF and suspended in Ringer-HEPES (6 mM $NaHCO_3$, 150 mM NaCl, 2.2 mM $CaCl_2$, 5.2 mM KCl, 0.2 mM $MgCl_2$, 5 mM HEPES and 2.8 mM D-glucose, pH 7,4) so that 200 µL contained 400 000 cells.

MAgEC 10.5 RT cells were seeded at a density of 30,000 cells per well in a 12-well plate and allowed to adhere for 12 hours. The medium was then replaced with serum-free Opti-MEM. After 6 hours, the cells were transfected with Lipofectamine 2000 and Fabs-encoding vectors (pl.DualCAG.Hygro.cAb2789 or pl.DualCAG.Hygro.cAb2508) according to the manufacturer’s instructions. Transfected cells were maintained in serum-free medium for an

additional 12 hours. After this period, hygromycin (125µg/mL) was added for selection. Following 24 hours of selection, the medium was replaced with fresh medium, which was changed every two days for two weeks. After two weeks, hygromycin-resistant colonies appeared. To isolate specific clones, the cells were detached and seeded at a density of one cell per well in a 96-well plate (1 cell/per well). The selected clones were screened for Fab secretion using western blot analysis.

4.2 Animals

Young, 8 to 12 weeks-old and old, 20 to 30 months-old female mice were used for aging experiments and 8-12 weeks old mixed sex for other experiments. Mouse strains used were: BALB/c and FVB/Ant:TgCAG-yfp_sb #27. Animal housing conditions complied with the laws of Hungary (article 40/2013. (II. 14.)), that conform European Union regulations: 22±2°C, 55±10% humidity, 25x air change per hour, 12-12 hours light-dark cycle with ad libitum access to regular chow and water. Cardboard tunnels were used for environmental enrichment. Procedures conformed to widely accepted standards, best practices and Hungarian laws of animal protection. The primary endpoint was MAgEC10.5 integration into brain vasculature. Group sizes were estimated using G*power when designing the experiments (version 3.1.9.7). To compare treatment groups, test family was set to "F tests", the statistical test used was "ANOVA: Fixed effects, omnibus, one-way", the type of analysis was "A priori: compute required sample size - given α, power and effect size. Effect size was determined from variances with "variance explained by special effect" set to 0.1 and "variance within group" set to 0.25. When comparing treatment groups over time, the statistical test used was “ANOVA: Repeated measures, within, between interactions”. For old mice, a 25% death rate was estimated. Individual mice were assigned to a list randomly, numbered for identification, and then placed into treatment groups. Experiments were not blinded, as individual experiments and their analysis were done by the same researchers. During the experiments, no confounders were identified. Animals were monitored daily for any indications for terminating the experiment such as infections, lethargy, greater than 25% loss of body weight, etc. In senolysis experiments, the number of young mice for 24 hours treatment were 6, 9, 7 while for 48 hours treatment were 7, 6, and 5 for control, abt-263, and dasatinib with quercetin groups respectively. Old groups had 5, 6, and 5 mice for 24-hour treatments and 5, 6, and 6 mice for 48 hours. EPC integration was checked in 2, 4, and 3 mice in the same groups as above after 5 days. For two-vessel

occlusion experiments, 5 groups of BALB/c animals were used with 3 animals in each of the 5 groups. TTC staining required 5 groups (MAgEC 10.5 injected and uninjected groups at two time points and a sham surgery group) and two groups were used to assess EPC integration. For *in vivo* BBB permeability, 15 MAgEC 10.5 cells were observed in 7 young mice and 5 cells in 3 old mice. For *in vivo* determination of EPC preactivation by TNFα 6 groups were used with 3 mice each (two time points with three treatment groups). A total of 105 BALB/c and 29 FVB/Ant:TgCAG-yfp_sb #27 mice were used. Euthanasia was carried out with the isoflurane overdose method by setting the evaporator to over 5% until breathing stopped.

Experiment	**Figure**	**Strain**	**Sex**	**Treatment**	**Number of mice**				
Senolytic	15B, D	BALB/c			Young		Old		
					24 hours	48 hours	24 hours	48 hours	5 days
			female	Control	6	7	5	5	2
			female	Abt-263	9	6	6	6	4
			female	D+Q	7	5	5	6	3
	15E				liver	kidney	spleen	Lung	Muscle
			mixed		2	2	2	2	2
Hypoxia (2VO)	14C	BALB/c			Vehicle		MAgEC-tomato		
					2 days	7 days	2 days	7 days	
			mixed		3	3	3	3	
	14D				Control	2VO			
			mixed		3	3			
BBB permeability					Young	Old			
	10B, C	FVB/Ant:TgCAG-yfp_sb #27	mixed		7	3			
TNF treatment					Control	1ng/ml	5ng/ml		
	9	FVB/Ant:TgCAG-yfp_sb #27	mixed		3	3	3		

Table 1. The number of mice used in experiments

4.3 Quantification of MAgEC10.5 adhesion and immunofluorescence

After 3, and 5 days, the animals were perfused with phosphate-buffered saline (PBS, 10 mM, pH = 7.4) and then fixed with 4% paraformaldehyde (PFA) in PBS for immunofluorescence. The brains were removed and postfixed in PFA at 4°C overnight. The next day, PBS was used instead of the fixative for the vibratome section, and the brains were

kept at 4°C until the next step. Following fixation, the whole brain was placed for coronal sectioning with a vibratome (VT1000 S, Leica Biosystems, Wetzlar, Germany). PBS with 0.05% sodium azide was used to preserve 30-um brain slices. Slices were incubated in PBS for 20 minutes at 85°C to perform antigen retrieval. 0.5% TritonX-100 in PBS was used for permeabilization for 1 hour at room temperature. Following that, blocking with 3% bovine serum albumin (BSA) in PBS was performed. The primary antibody solutions were prepared in PBS with 3% BSA.

Under slow nutation, sections were incubated overnight at 4°C. The following primary and secondary antibodies are shown in Table 1. Sections were thoroughly rinsed in PBS before exposure to the secondary antibody solution for 60 minutes at room temperature in the dark. The sections were counterstained with color-compatible nuclear staining (Hoechst 33342, Sigma-Aldrich) for 5 minutes, washed with PBS, and mounted with FluoroMount-G medium (Southern Biotech, USA). A fluorescent microscope (Axiovert Z1, Zeiss, Budapest, Hungary) equipped with super-resolution capable laser scanning confocal microscopy (Stedycon, Abberior Instruments, Göttingen, Germany) was used to record immunofluorescence.

Primary Antibody	Cat. No	Application
anti-claudin-5 m.	35-2500, Invitrogen, ThermoFisher, Waltham, USA	IF: 1:200 in 3% BSA in PBS
anti-AQP4 m	sc-390488, Santa Cruz Biotechnology, Dallas, USA	IF: 1:200 in 3% BSA in PBS
anti-collagen IV	Abcam, Cambridge, UK, #ab6586	IF: 1:200 in 3% BSA in PBS
anti-Fab m	Sigma Aldrich, #A182	IF: 1:200 in 3% BSA in PBS
anti-PECAM-1	NB100-2284, Novus Biologicals, Centennial, CO, USA	IF: 1:100 in 3% BSA in PBS
Secondary Antibody	**Cat. No**	**Application**
Alexa Fluor® 594 AffiniPure g. anti-mouse IgG (H + L)	115-585-003 (Jackson Immuno Research, Ely, UK)	IF: 1:500 in 1% BSA in PBS
Alexa Fluor® 647 AffiniPure g. anti-rabbit IgG (H + L)	111-605-003 (Jackson Immuno Research)	IF: 1:500 in 1% BSA in PBS
Alexa Fluor® 488 Cross-Adsorbed d. anti-goat IgG (H + L)	A-11055 (Thermo Fisher Scientific	IF: 1:500 in 1% BSA in PBS

g. = goat, m. = mouse, r. = rabbit, IF = immunofluorescence.

Table 2. Primary and secondary antibodies used

4.4 Two-photon imaging

Intravital, two-photon imaging was performed as previously described (Tóth et al., 2021). Mice were placed on a heating system after being given isoflurane anesthesia. Anesthesia was induced with 4% isoflurane and maintained with 1.5% using an isoflurane evaporator (RWD, Guangdong, China). The attached aluminum bar immobilized and held the head in place. Due to the superficial pial vasculature's consistent placement and recognizable pattern, we could capture the same cortical volume over days. Intravenous microscopy was conducted with a FEMTO 3D Dual microscope (Femtonics, Budapest, Hungary) using a 20x extended working distance water immersion objective (XLUMPLFLN-20XW, Olympus) and MES software (v6, Femtonics, Budapest, Hungary). A Mai Tai HP Ti-sapphire laser (RK TECH Ltd.) was used to optimize Venus-YFP and tdTomato. This laser was also sufficient for SR101 and optimum for EmGFP and CellTracker Red CMTPX excitation. The laser power was varied between 10% and 40% depending on the imaging depth (0–400μm from the brain's surface). GaAsP photomultipliers were used to acquire emission wavelengths. For the first 24 hours after inoculation, larger volumes (x: 500μm, y: 500μm, and z: 250 μm) were recorded with three μm vertical steps to assess cell number changes and dynamics of EPCs cell integration. Image stacks were automatically merged, leveled, and RGB-converted in Fiji (software versions: ImageJ154f and Java 1.8.0_66 64bit).

4.5 Cranial window

Cranial windows were implanted similarly to previously described (Haskó et al., 2019). Before and throughout the surgery, animals were administered 1-2% isoflurane gas (RWD, Guangdong, China) through inhalation using a Surgivet Classic T3 vaporizer (RWD, Guangdong, China), set at a flow rate of 1-2 liters per minute. The depth of anesthesia was assessed by monitoring toe, tail pinch reflexes, and eye blink. During the operations, the experimental animal was placed on a heating pad (RWD, Guangdong, China) to maintain a constant temperature. Ear and nose bars secured the animal's head in a stereotaxic frame adapter. Eye ointment was applied to both eyes to prevent dryness, and a hair removal cream was administered to the head. Subsequently, the area was disinfected using 70% ethanol, and the skin on the top of the head was removed. The periosteum was irrigated with a 2% Lidocaine solution (Sigma-Aldrich, St. Louis, MO). To ensure a clean surface, the periosteum was carefully scraped away from the exposed region of the cranium, followed by a thorough

washing of the area. Using an OM-6 operating microscope (Takagi, Tokyo, Japan), the skull was gently thinned across the sensorimotor cortex in a 3–4 mm diameter region using a micro drill (H.MH-170, Foredom, Blackstone Industries, Bethel, Connecticut, USA). The centers for the craniotomies were approximately 1.7 mm posterior and 2.2 mm lateral from the bregma. During this process, sterile Ringer-HEPES cold drops were applied to cool the surface, and debris was removed using compressed air. Once the bone reached the desired thinness, as indicated by slight movement upon gentle pressure, a craniotomy was performed using a drop of sterile Ringer-HEPES solution. A gelatin sponge soaked in sterile Ringer-HEPES solution was employed to control any unintentional hemorrhage resulting from the craniotomy. A 5 mm-diameter coverslip (Thomas Scientific, Swedesboro, NJ) was placed over the exposed brain, and Cyanoacrylate glue was used to seal the glass's edge. An aluminum head plate was cemented to the skull. After the procedure, mice were intraperitoneal injected with Rimadyl (carprofen, 5mg/kg) and were left to convalesce to reduce inflammation from the surgery. A one-month healing interval was observed between cranial window implantation and intravital microscopy observation (Figure 2)

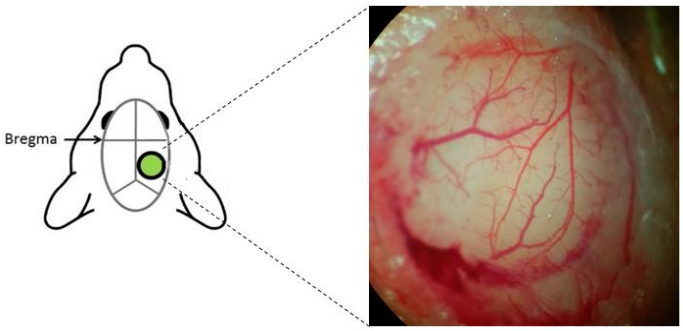

Figure 2. Cranial window after 3 weeks of implantation

4.6 Intracarotid injection

Intracarotid injections were performed as previously described (Haskó et al., 2019). Before surgery, all surgical instruments and supplies were sterilized. Anesthesia was induced with 4% isoflurane and maintained with 1.5% using an isoflurane evaporator (RWD, Guangdong, China). The animal's feet were gently pinched to ensure complete sedation, and no reaction was observed. The mouse was then securely positioned on a heated pad using rubber bands. The neck area was shaved or treated with a hair removal solution, then the hair was removed with a paper towel.

Next, povidone-iodine and 70% alcohol were applied to clean the skin of the neck. The mouse was positioned on the stage of the dissecting microscope (Takagi OM-6). A surgical scalpel was used, and a small incision, less than one centimeter long, was made in the skin. Toothed forceps were used to dissect through the muscle, exposing the carotid artery beneath. Surgical forceps were employed to separate the carotid artery from the adjacent vagus nerve. A small cotton ball, moistened with Ringer-HEPES, was placed under the carotid artery at the injection site. Loose knots were tied distally and proximally to the cotton ball, with the proximal knot tightened to prevent blood from entering the injection site. Cell injection was performed once the carotid artery on the cotton ball appeared to be fully compressed with fresh red blood.

A volume of 200µl of MAgEC cells was vortexed and drawn into a 1 ml syringe (Inject F Braun). Slowly, a 30G needle (BD Microlance 3) was inserted into the lumen of the carotid artery, positioned over the cotton ball, under the dissecting microscope. The cells were then slowly administered through the carotid artery (Figure 3). The successful injection was confirmed by observing the morphology of nearby blood vessels and muscles under the microscope. After the injection, the distal carotid artery was gently lifted to prevent regurgitation. The muscle was repositioned to cover the incision site, and the skin was closed using glue.

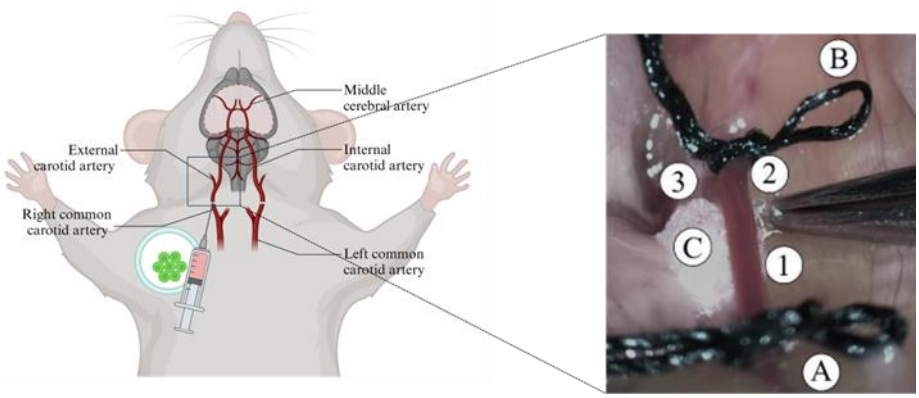

Figure 3. Intracarotid injection

The right common carotid artery (**1**) and two of its branches, the external carotid artery **(2**) and internal carotid artery (**3**). Temporary ligations were made at the proximal part (**A**) of the common carotid artery and at the external carotid artery (**B**). A moist cotton ball was used to lift the common carotid (**C**)

4.7 Femoral artery cannulation and fluorescent tracer injection

Anesthesia was induced with 4% isoflurane and maintained with 1.5% using an isoflurane evaporator (RWD, Guangdong, China). The inner thigh of the mouse was shaved

and disinfected with 70% ethanol and iodine. The skin was cut parallel to the femur, and connective tissue was retracted. Under an OM-6 operating microscope (Takagi, Tokyo, Japan), the femoral artery, vein, and nerve were separated bluntly. The artery was lifted from the tissue by placing three pieces of surgical thread, and three ligatures were placed. The distal ligature was tightened permanently, and the proximal was tightened temporarily. A small cut was made on the artery with micro scaffolds, through which the cannula was inserted and fixed in position with the middle ligation and the remaining thread of the distal one. The proximal ligature was opened to gain access to the circulation, and the skin was closed. Throughout the operation, the area was irrigated with sterile Ringer-HEPES (Figure 4).

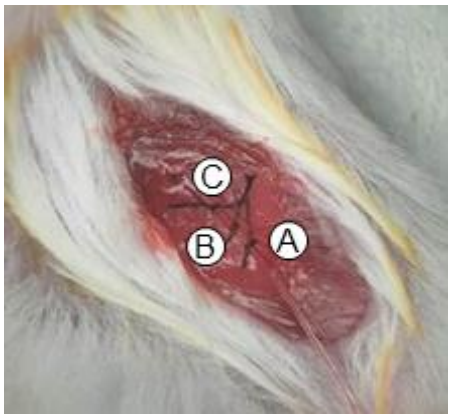

Figure 4. Femoral artery cannulation

(**A**) Distal ligature tightened permanently. (**B**) Proximal ligature tightened temporarily. The cannula (arrow) was inserted and fixed in position with the middle ligation (**C**)

4.8 Two-Vessel Occlusion (2VO)

Briefly, anesthesia was induced with 4% isoflurane and maintained with 1.5% using an isoflurane evaporator (RWD, Guangdong, China). A 0.5-1 cm vertical skin incision was made along the ventral midline of the neck. The fat and connective tissue were lifted using forceps to access the tissue plane underneath. While observing through the microscope, the common carotid artery (CCA) was carefully separated from the surrounding nerves and veins using forceps. This procedure was repeated for both CCAs. The CCAs were gently pulled up through the silk suture and clipped with microclamps. The isoflurane concentration was reduced to 1%, ensuring the mouse did not react when its tail was pinched. After 30 minutes, the clips and silk sutures beneath the CCAs were removed. Finally, glue was applied to the skin wound to seal it (Figure 5).

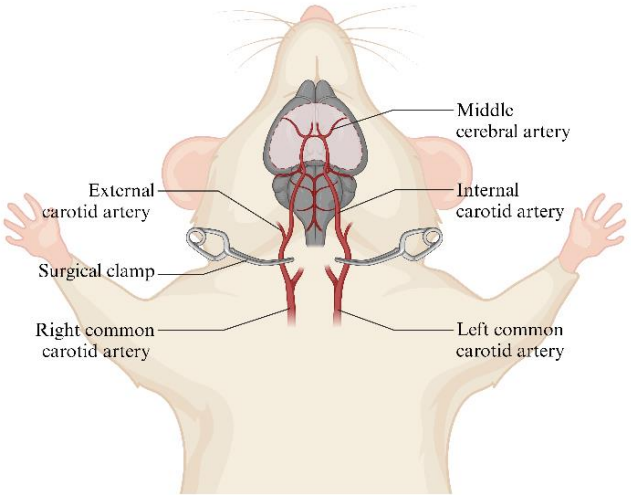

Figure 5. Two-Vessel Occlusion (2VO) mouse model

4.9 2,3,5-triphenyltetrazolium chloride (TTC) staining

The brains were rapidly isolated and placed in cold PBS (0-4°C). Using a vibratome (VT1000 S, Leica Biosystems, Wetzlar, Germany), the brains were sectioned into 450µm-thick coronal slices within 10 minutes post-decapitation. The brain slices were then immersed in TTC solution (10ml, 2% TTC in PBS) for 10 minutes at 37°C. Following staining, the slices were fixed in 4% formaldehyde solution. Metabolically active regions stained red, whereas cerebral infarctions remained white. The sections were photographed using a Takagi OM-6 operating microscope, and infarct volumes were measured using FIJI software.

4.10 TNFα pre-treatment of MAgEC 10.5-tomato cells

MAgEC 10.5-tomato cells were seeded at 500 000 cells per 3.5 cm diameter culture dish. The following day, the cells were treated with 1 or 5 ng/mL rmTNFα (Peprotech, Margravine Road, London, UK) for 1 hour in serum-free OPTIMEM I before injection into the carotid artery of mice. To minimize the negative effects of TNFα, we selected these low doses and short treatment of the endothelial progenitor cells over systemic treatment of the mice.

4.11 Quantification of MAgEC10.5 integration

Formaldehyde-fixed 30 µm brain sections from control and 2VO mice were imaged using a fluorescent microscope (Axiovert Z1, Zeiss, Budapest, Hungary) equipped with a digital camera and managed by the micro-manager software (D. Edelstein et al., 2014; Edelstein et al., 2010). Cells were categorized based on their morphology: solid, bright cells that visibly filled

the vessel lumen were classified as adherent, whereas cells exhibiting clear endothelial morphology, characterized by thin cells surrounding the lumen with a thicker central region containing the nucleus, were counted as integrated. This classification was straightforward for vessels aligned parallel or nearly parallel with the sectioning plane; however, determining the morphology was challenging for vessels oriented perpendicular or nearly perpendicular to the brain section.

4.12 Senolysis

Both young and aged BALB/c mice were administered senolytics dissolved in a vehicle mixture consisting of 60% Phosal 50 PG (Lipoid AG), 30% polyethylene glycol 400, and 10% ethanol (Molar Chemicals Kft, Budapest, Hungary). The first treatment protocol involved administering 100 mg/kg Abt-263 (MedChemexpress, Monmouth Junction, New Jersey, USA) once daily for five days via oral gavage. The second protocol involved a single oral gavage of 5 mg/kg dasatinib (Sellekchem, Houston, Texas, USA) combined with 50 mg/kg quercetin. Control groups received the vehicle mixture alone. Seven days post-treatment initiation, the mice were injected with MAgEC 10.5-tomato cells through the internal carotid artery.

4.13 *In vivo* BBB permeability measurement

Young and old FVB/Ant: TgCAG-yfp_sb#27 mice underwent cranial window implantation for two-photon microscopy and were injected with MAgEC 10.5-tomato cells. Mice displaying red fluorescent MAgECs within the cranial window two days post-injection were then cannulated in the femoral artery and repositioned under the two-photon microscope. They were subsequently injected with Na-fluorescein and Evans blue, serving as low and high molecular weight tracers, respectively, through the cannula. Fluorescence intensity for the tracers was measured in two-photon images in regions of interest (ROI) near blood vessels containing MAgEC 10.5-tomato cells and in control vessels without them. Given the average distance between brain capillaries is approximately 40µm, one ROI was selected immediately adjacent to the vessel, while the second was placed 20µm away. The second ROI was chosen in a way that no other vessel was closer to it on the basis of previous three-dimensional imaging.

4.14 Statistical analysis

Data for each group were tested using the Shapiro-Wilk test of normality (shapiro.test()) and outliers for outliers (identify_outliers()) then ANOVA with post hoc Tukey test was

performed using R and R Commander (versions 4.3.1 and 2.8-0). T-tests were calculated in Excel (Microsoft Office 2016). Data are presented in standard box plots or bar graphs of means with standard deviations, as specified in the figure legends. Statistically significant differences were indicated with their respective significance levels. All animals and measurements were included in the study.

5. RESULTS

5.1 MAgEC10.5 EPC adhesion to the brain vasculature

MAgEC 10.5 immortalized EPCs, labeled with CellTracker Red or red fluorescent MAgEC 10.5-tomato cells were cultured sparse (Figure 6A) to avoid cell clumping when injected through the internal carotid artery (ICA) of young BALB/c mice. The injected cells rapidly adhered to the vasculature and, thus most of the observed cells were in the ipsilateral hemisphere (Figure 6B). In brain sections, the progenitor cells were seen inside capillary vessels and appeared to fill the lumen. However, the microvessels were likely not completely blocked, as we did not see blood cells stuck next to the progenitors in the vessel lumens after transcardial perfusion or during *in vivo* microscopy. Immunofluorescence labeling of neurovascular unit components, such as the collagen IV in the basal membrane allowed the monitoring of the MAgEC 10.5 endothelial progenitor cell adhesion and integration within the vessels (Figure 6C).

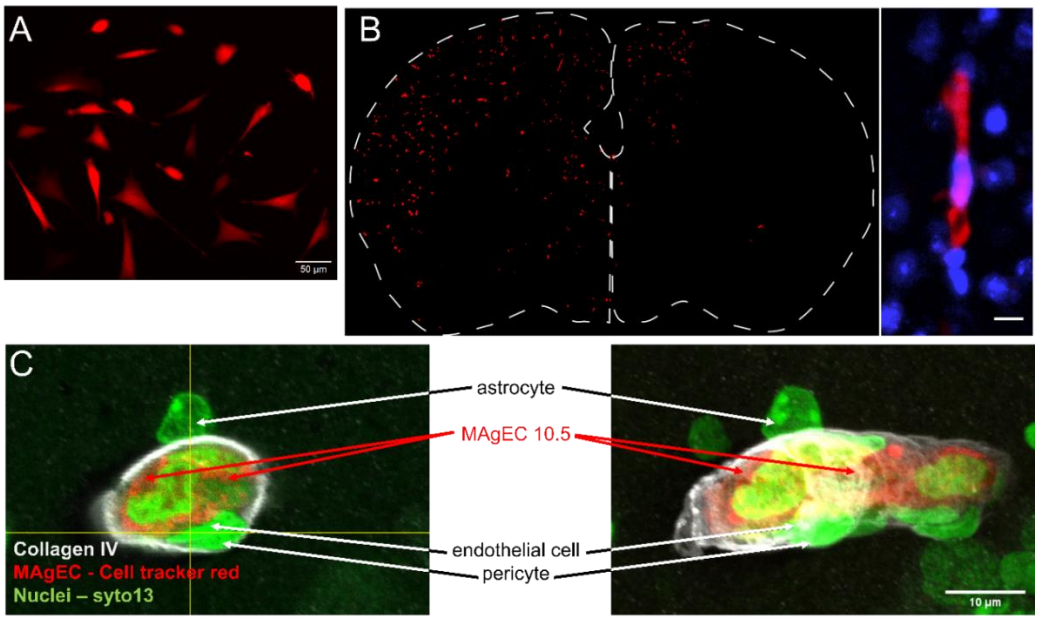

Figure 6. MAgEC 10.5 EPC adhesion in brain vessels

A Sparse culture of MAgEC 10.5 cell line displaying tdTomato expression (red), bars are 50µm . **B** MAgEC 10.5-tomato cells were injected in BALB/c mice and were observed *ex vivo* in the ipsilateral hemisphere one day after injection. Right panel: an example of adherent red fluorescent progenitor cell. Nuclei labeled blue with Hoechst 33342, bars are 10µm . **C** Microscopic detection of MAgEC 10.5 cells labeled with CellTracker Red. Syto 13 (green), a nuclear stain, was used to approximate cell identification based on the position and shape of the nuclei. This allowed for the identification of astrocytes, pericytes endothelial cells in the vessel walls, and MAgECs inside the vessels. Collagen IV staining highlighted the extracellular

matrix, aiding in determining the relative position of MAgECs inside the vessels and their localization in the brain microvasculature, bars are 10µm.

Monitoring MAgEC 10.5-tomato cells through cranial windows in FVB/Ant:TgCAG-yfp_sb #27 mice that express Venus yellow fluorescent protein in endothelial cells, we observed that at this point, some of the red fluorescent MAgEC 10.5-tomato stay at the same location for 24 hours or even 5 days or longer (Figure 7A), while others detached and moved to different sites (Figure 7B).

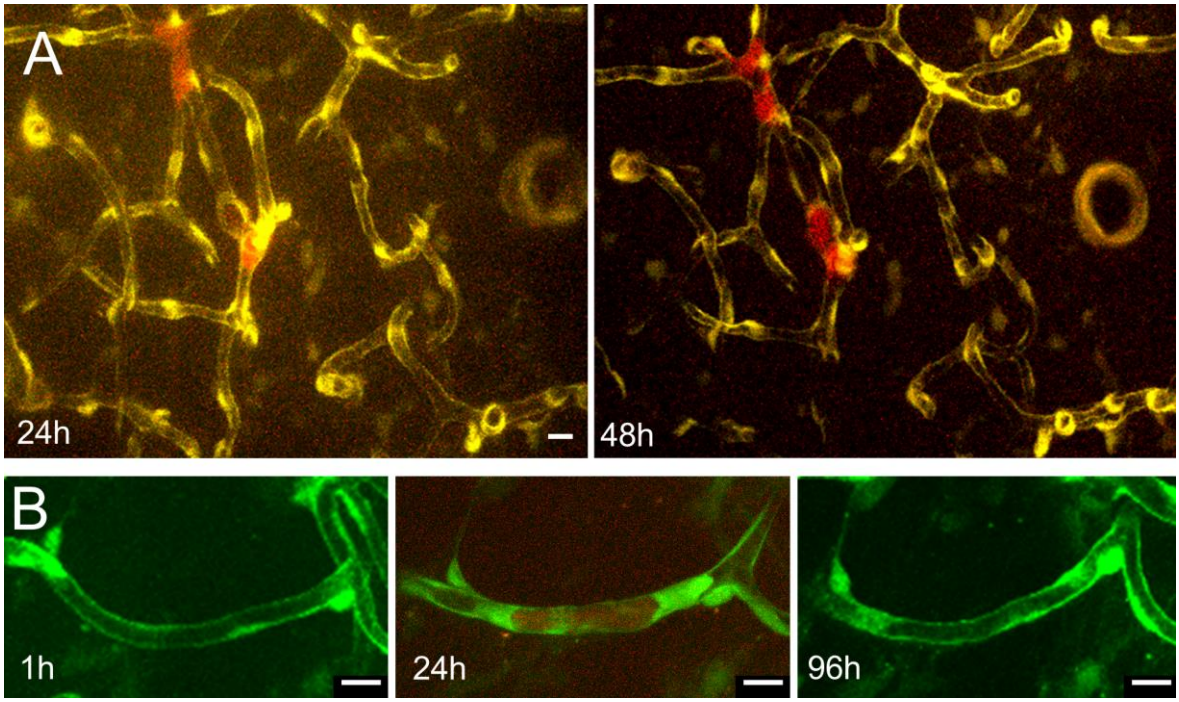

Figure 7. MAgEC 10.5 EPC adhesion in brain vessels *in vivo*

MAgEC 10.5-tomato were followed *in vivo* in the somatosensory cortex of FVB/Ant:TgCAG-yfp_sb #27 mice using two-photon microscopy, having vascular endothelial cells labeled in yellow. **A** Representative progenitor cells (red) stayed at the same location 24 and 48 hours after injection. **B** Representative progenitor cell (red) was not present 1H after injection and was adherent to the vessel at 24 hours and moved 96 hours after injection. Bars are 10 µm.

5.2 MAgEC10.5 EPC cell integration into the capillary bed

MAgEC 10.5 immortalized EPCs, labeled with CellTracker Red, were injected into the common carotid artery of adult wild-type BALB/c mice. As early as 28 hours post-injection, the EPCs were observed flattening along the vessel walls (Figure 8A), suggesting that these cells were potentially at an early step of integration into the vessel wall. For longer-term studies, MAgEC 10.5 cells were modified to express the red fluorescent protein, creating the MAgEC

10.5-tomato line, and similarly injected into BALB/c mice. Seven days after injection, the cells were analyzed for claudin 5, a tight junction protein marker. The results demonstrated the formation of tight junctions between the injected MAgEC 10.5-tomato cells and the unlabeled resident endothelial cells (Figure 8B, C). We concluded that the presented MAgEC 10.5-tomato cells were integrated into the capillary bed though we could only observe a partial vessel lumen as the vessel was bisected during sectioning. Later, by monitoring MAgEC 10.5-tomato cells in young BALB/c brain tissue after injection, we found that multiple cells took up endothelial-like morphology within five days. Immunofluorescence labeling and laser confocal microscopy revealed that MAgECs integrated into the capillary bed, presenting continuous tight junctions (TJs) visualized by claudin 5 staining and forming the vessel lumen together with preexisting endothelial cells (Figure 8D). The existence of TJs between the MAgEC 10.5-tomato derived and pre-existing cells and the presence of a vessel lumen strongly suggest that these are functional blood vessels (Figure 8E).

To support our *ex vivo* findings, we monitored MAgEC 10.5-tomato interactions with brain vasculature *in vivo*. MAgEC 10.5-tomato cells were injected into adult wild-type BALB/c mice, which previously underwent cranial window surgery. During this procedure, a clear glass plate was implanted into the parietal bone to allow for intravital two-photon imaging of brain tissue. 3D volume scanning with a two-photon microscope was used to monitor the integration of MAgEC 10.5-tomato cells into brain endothelial cells *in vivo*. Even though integration is not a common event and the brain volume that can be monitored is restricted to an approximately 3mm circular area and a depth of 200-400µm, we successfully observed an integrated MAgEC 10.5-tomato cell integrated into the cortical microvasculature (Figure 8F). During the observation blood flow through the tdTomato positive vessel segment was clearly visible due to Cascade Blue dextran labeling.

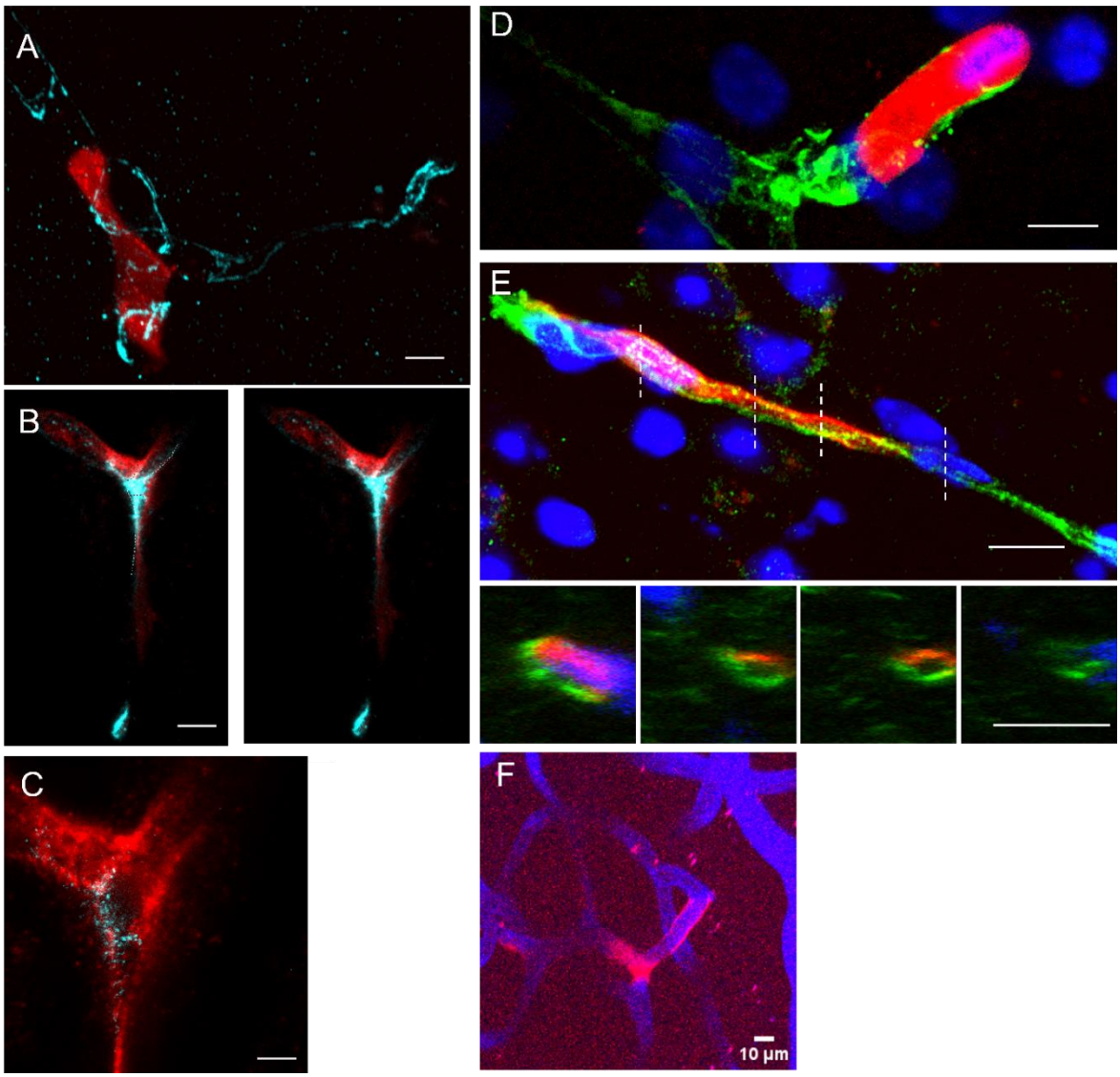

Figure 8. MAgEC 10.5 EPC integration into the capillary bed

MAgEC 10.5-tomato cells were injected into BALB/c mice. **A**. At 28 hours following ICA injection of MAgEC 10.5 (Cell tracker red labeled, red), some EPCs were observed in the brain microvasculature without completely obstructing the vessel lumen. The brain capillaries were delineated using PECAM-1 immunolabelling (cyan). The image represents a maximum intensity projection of a confocal z-stack. **B**. Seven days post-ICA injection, transduced MAgEC 10.5-tdTomato cells (red, immunolabelled with anti-RFP) were observed integrated into the brain vasculature. In one capillary branch, an endothelial cell derived from the transduced EPC appeared to line the lumen. In another branch, the vessel wall was partially made up by a red fluorescent cell. Claudin 5 immunolabeling (cyan) indicated tight junctions between two regions of the same EPC-derived endothelial cell in both upper branches, as well as between an EPC-derived endothelial cell (red) and an unlabelled endothelial cell (white dashed lines). Tight junctions encircled adjacent endothelial cells, sealing the connection between them (black dashed lines). The right panel shows the image without overlay. The image is the maximum intensity projection of a confocal z-stack. **C** STED image from a single optical section of the stack reveals the tight junction strand structure at higher resolution (40 nm pixel

size). Immunofluorescent labeling of claudin 5 in green shows: **D.** MAgEC 10.5-tomato cell in the lumen of a brain microvessel and **E.** MAgEC 10.5-tomato cell differentiated into an endothelial cell and integrated into the wall of a microvessel observed in the thalamus. Orthogonal images taken at the dashed lines reveal the vessel lumen formed by the MAgEC 10.5-tomato derived endothelial cell and a preexisting endothelial cell together. **F** *In vivo* two-photon microscopic image of MAgEC 10.5-tomato integrated into the microvasculature (red: MAgEC 10.5-tomato cell, Blue: Cascade Blue-dextran vascular label). Bars are 10 µm.

5.3 *In vivo* EPC adhesion and integration after preactivation by TNFα

Theoretically, the positive effect of EPCs on tissue regeneration can be enhanced by increasing the number of progenitors that adhere to the brain vasculature. As TNFα activates EPC adhesion *in vitro* (Prisco et al., 2015), we pre-treated MAgEC 10.5-tomato cells in culture for one hour with 1 or 5ng/mL TNFα before injecting them in FVB/Ant:TgCAG-yfp_sb #27 mice. Using intravital two-photon microscopy, we saw an increased number of adherent cells 24 hours after injection. Monitoring the adherent cells for 120 hours, we found that a larger number of individual cells stayed at the same location in the vasculature compared with untreated controls (Figure 9).

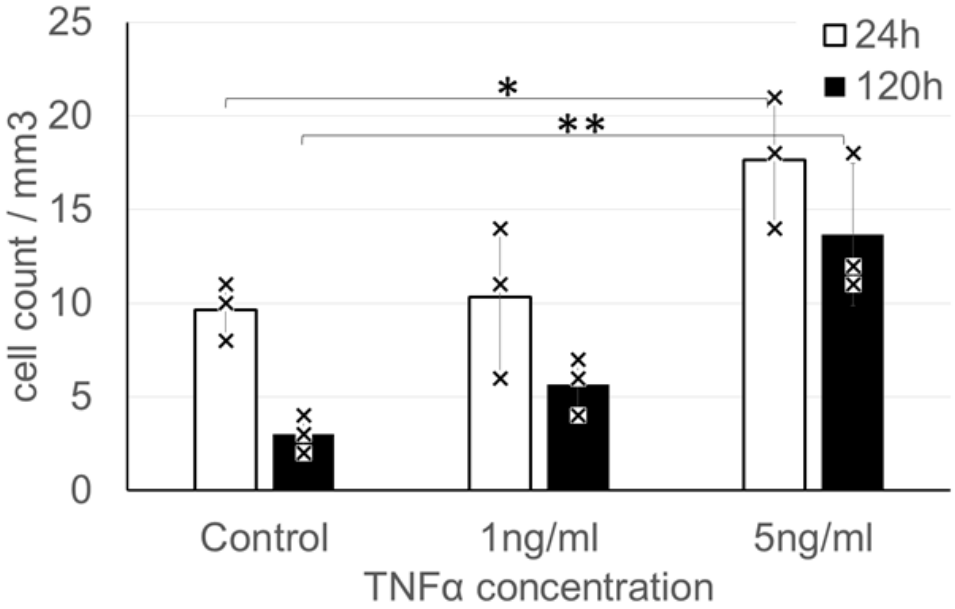

Figure 9. Effect of TNFα on EPC adhesion *in vivo* in young BALB/c mice

Based on intravital two-photon imaging, MAgEC 10.5-tomato cells pre-treated with TNFα adhered to vasculature in greater numbers 24 hours after injection. Revisiting the same cells after 120 hours shows that more cells stayed at the same location if pre-treated with TNFα. Means +/- standard deviation are presented, n=3 for each group, ANOVA: * $p \leq 0.05$, ** $p \leq 0.01$

5.4 *In vivo* BBB function at EPC adhesion sites

To learn whether the arrest of EPCs induces changes in vascular functionality, functional assessment of the BBB and the TJs was performed by monitoring *in vivo* permeability using intravital two-photon microscopy. Young and old FVB/Ant: TgCAG-yfp_sb #27 mice underwent cranial window implantation for two-photon microscopy. The mice were injected with MAgEC 10.5-tomato. Mice in which red fluorescent MAgECs were present within the cranial window two days after injection were then cannulated in the femoral artery, placed back into the two-photon microscope, and injected with Na-fluorescein and Evans blue as low and high-molecular-weight tracers through the cannula. Fluorescence intensity for the tracers was measured in two-photon images in regions of interest (ROI) near blood vessels containing MAgEC 10.5-tomato cells and control vessels that did not. The average distance between capillaries in the brain is approximately 40µm, thus one ROI was chosen immediately next to the vessel, while the second one was placed 20µm farther. The second ROI was chosen in a way that no other vessel was closer to it based on previous three-dimensional imaging (Figure 10A). ANOVA analysis showed that the BBB permeability for Na-fluorescein (Figure 10B, C) and Evans blue-albumin (not shown) did not significantly change either in young or old mice two days after the injection of cells. We also did not observe a gradient between the ROI closer or farther away from the vessel in question.

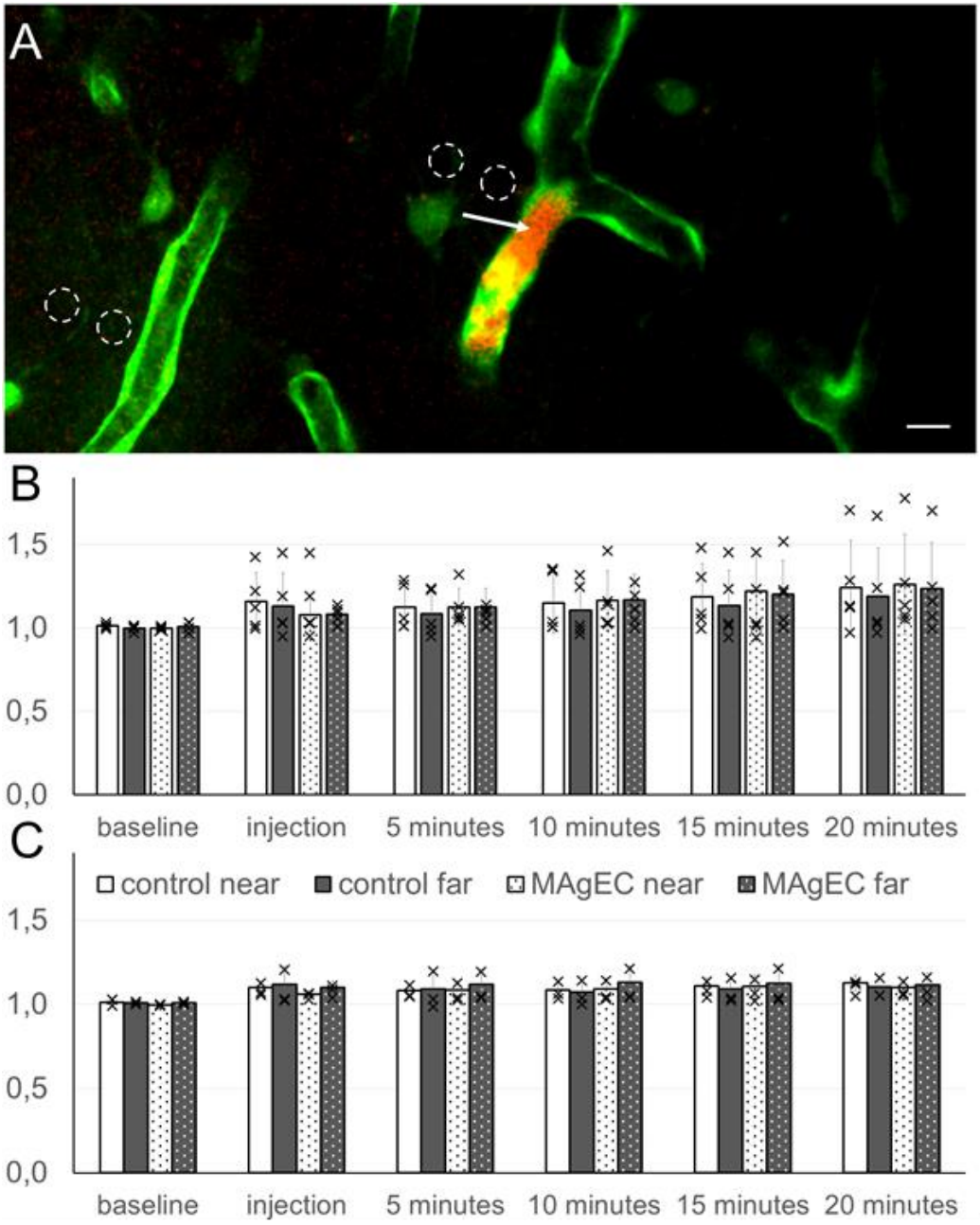

Figure 10. *In vivo* BBB permeability measurements at MAgEC 10.5 EPC adhesion sites

Two days after injecting MAgEC 10.5-tomato in FVB/Ant:TgCAG-yfp_sb #27 mice, vascular permeability was assayed *in vivo* near MAgEC 10.5 cells in the somatosensory cortex. **A** Example maximum intensity projection for the location of ROIs (circles) for fluorescence measurement near a MAgEC cell marked with the arrow and at a control vessel. The intensity measurements were done on single optical sections. Bar is 10µm. **B** and **C** Bar graphs show relative fluorescent intensity over time next to or farther away from vessels, that either contained a MAgEC 10.5-tomato cell or not in the brain of B young or C old mice. Means +/- standard deviation are presented, n=5 for young and n=3 for old.

5.5 Detection of EPC secreted Fab in the brain

Given that MAgEC EPCs closely associated with the brain vasculature, we tested whether these cells could be used as vectors for treating neurological disorders after genetic modification for the secretion of therapeutic molecules. Therefore, MAgEC 10.5 cells were further modified to also express the anti-TDP-43 Fab (cells named MAgEC 10.5 RT anti-TDP-43). Following the characterization of the cells and carotid injection into BALB/c mice, immunolabelling was used to localize the MAgEC 10.5 RT anti-TDP-43 cells and the anti-TDP-43 Fab expressed in relation to the brain microvasculature. The anti-TDP-43 Fab was detected in EPCs located in the brain vasculature 7 days after injection (Figure 11A). Furthermore, anti-TDP-43 Fabs were also observed outside PECAM-1 labeled microvessels that contained red fluorescent EPCs expressing this Fab (Figure 11B). To test whether the Fab localized into the perivascular space and penetrated the brain parenchyma, we immunolabelled astrocytic endfeet that ensheathe the microvasculature by its specific marker aquaporin-4. We observed a distinct localization of the Fabs along the aquaporin-4 stained endfeet (Figure 11C). From these images, it was not possible to differentiate the luminal and abluminal sides of astrocytic endfeet even using super-resolution microscopy (Figure 12). Nevertheless, we observed sites where the Fabs were clearly localized in the brain parenchyma, past the aquaporin-4 signal. Notably, some extravascular anti-TDP-43 Fab co-localised with tdTomato originating from MAgEC 10.5 RT anti-TDP-43 cells, suggesting vesicular localization (Figure 13).

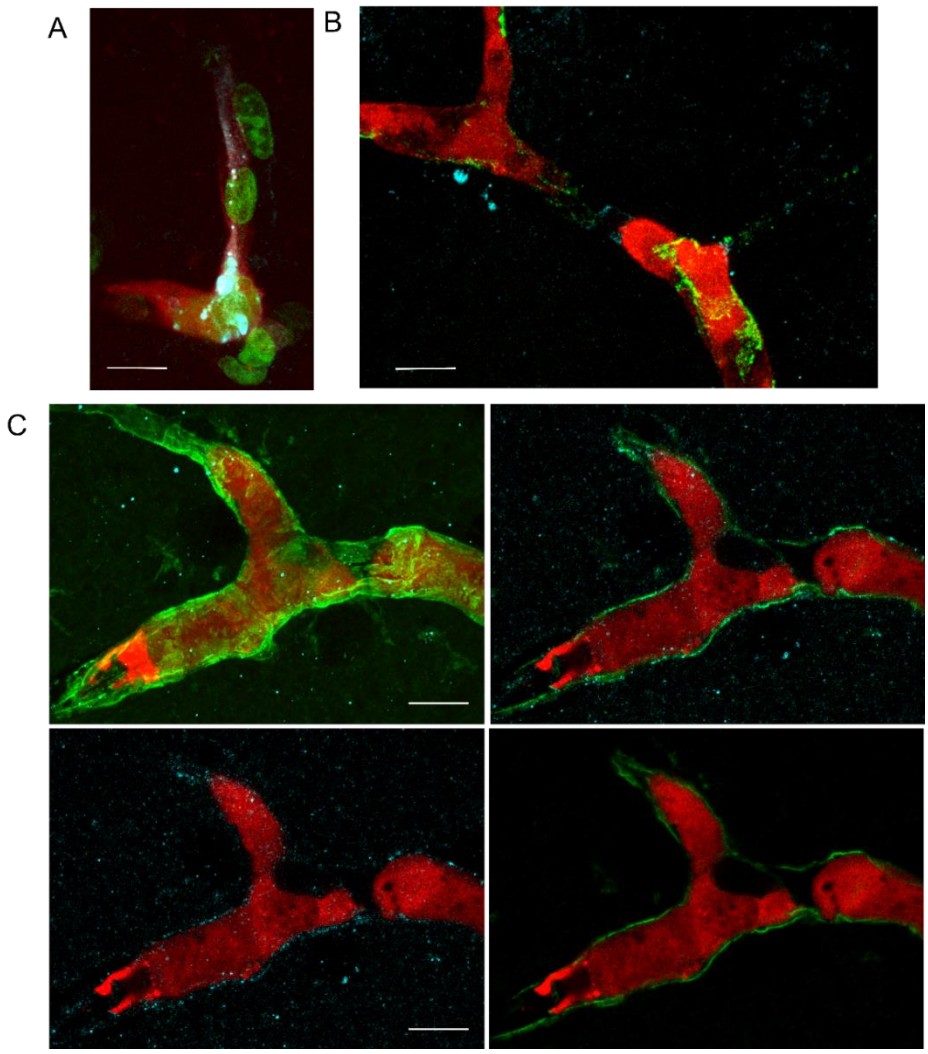

Figure 11. Therapeutic antibody production and localization *in vivo*

Exogenous TDP-43 antibody secreted by MAgEC cells was visualized in the brain vasculature and parenchyma using confocal and super-resolution microscopy. **A.** Seven days post-injection, MAgEC 10.5 anti-TDP-43 cells (tdTomato, red) secreting anti-TDP-43 Fab fragments (cyan, white in co-localization with red) in mouse brain tissue, with nuclei stained by Syto-13 (green). Image is a confocal maximum intensity projection. **B**. At 48 hours, anti-TDP-43 Fab fragments (cyan) produced by MAgEC cells (red) crossed the blood-brain barrier, localizing outside microvessels labeled with anti-PECAM-1 (green). **C.** Fab localization at the astrocytic endfeet (aquaporin-4, green). The first panel is the maximum intensity projection, subsequent panels present a single optical section showing all channels, MAgEC cells and TDP-43 Fab staining, MAgEC cells and aquaporin-4 staining, respectively. Scale bars are 10 μm.

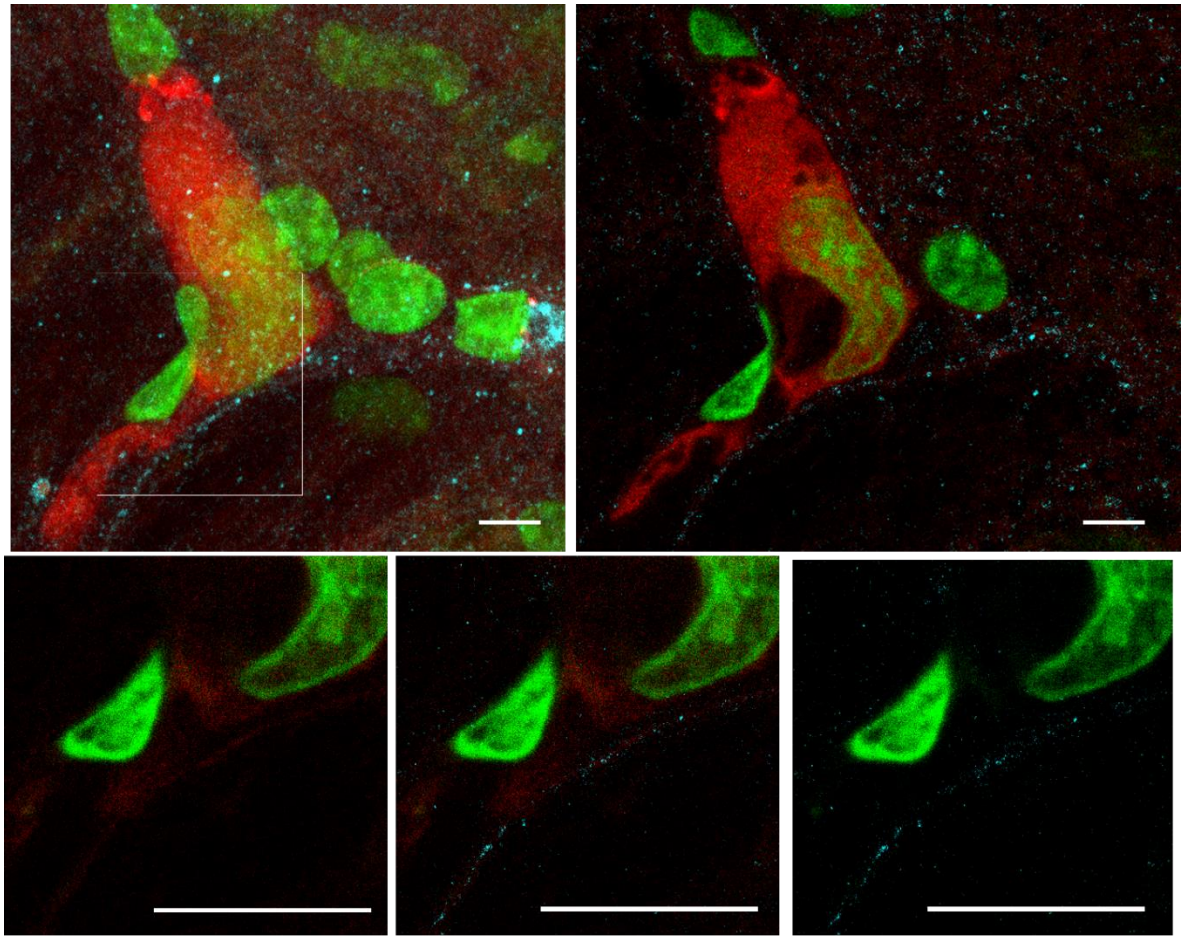

Figure 12. Therapeutic antibody localization via STED superresolution microscopy

The first two larger panels present confocal maximum intensity projection and single optical section of a brain microvessel containing MAgEC 10.5 RT anti-TDP-43 cells. In this case aquaporin-4 was stained red to allow simultaneous STED imaging with the TDP-43 Fab (cyan). The smaller panels show STED images of the area marked with a white square. On most images, it is hard to conclude whether the Fab signal is on the luminal side or the abluminal side of astrocytic end-feet even using super-resolution microscopy. The scale bars are 10 μm.

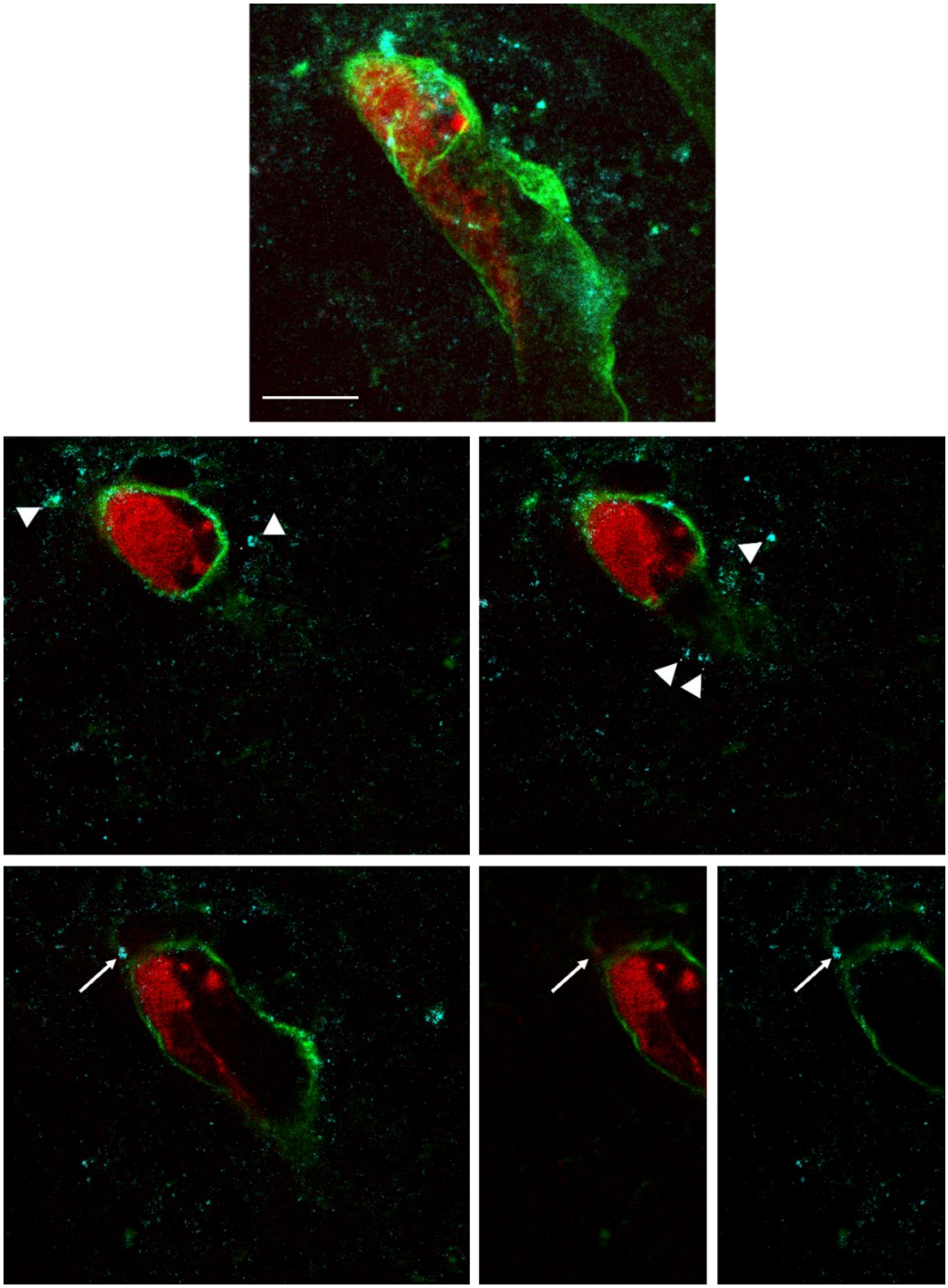

Figure 13. Therapeutic antibody detection in the brain parenchyma

Fab signal (arrowheads) that clearly localized in the brain parenchyma outside microvessels containing MAgEC 10.5 anti-TDP-43 cells. The parenchymal TDP-43 Fab staining, past the aquaporin-4 signal coincided with red signal from tdTomato originating from MAgEC cells (arrow). The image shows a maximum intensity projection in the first panel, single optical sections in the following panels, and the last two panels show aquaporin (green) or TDP-43 Fab (cyan) beside the MAgEC cells. The scale bar is 10 µm.

5.6 Effect of hypoxia on EPC integration and tissue regeneration *in vivo*

As tissue damage induced by ischemic injury can be alleviated by EPC treatment, we used an experimental hypoxia model to study the role of EPC integration in this. BALB/c mice underwent two-vessel occlusion (2VO), which causes mild ischemic stroke in the anterior circulation) before being injected with MAgEC 10.5-tomato to model global hypoxia. The initial ipsilateral distribution of MAgEC 10.5-tomato cells in healthy brains shifted to a uniform distribution across both hemispheres in hypoxia (Figure 14A). The extent of the injury was measured by comparing the area showing tissue damage to the whole area of brain sections on photographs after TTC staining (Figure 14B). Injecting MAgEC 10.5-tomato resulted in significantly greater recovery of the ischemic tissue. Two days after ischemic insult, the injured brain tissue volume was 22 and 21 % for sham and MAgEC 10.5-tomato injected animals, whereas, after 7 days, it decreased to 17 and 11 %, respectively (Figure 14C). To determine the effect of hypoxia on EPC integration, we counted MAgEC 10.5-tomato cells in tissue sections five days after 2VO and EPC cell injection. We observed a significant, approximately twofold increase in the total and integrated number of MAgEC 10.5-tomato cells in response to 2VO compared to sham-operated controls (Figure 14D).

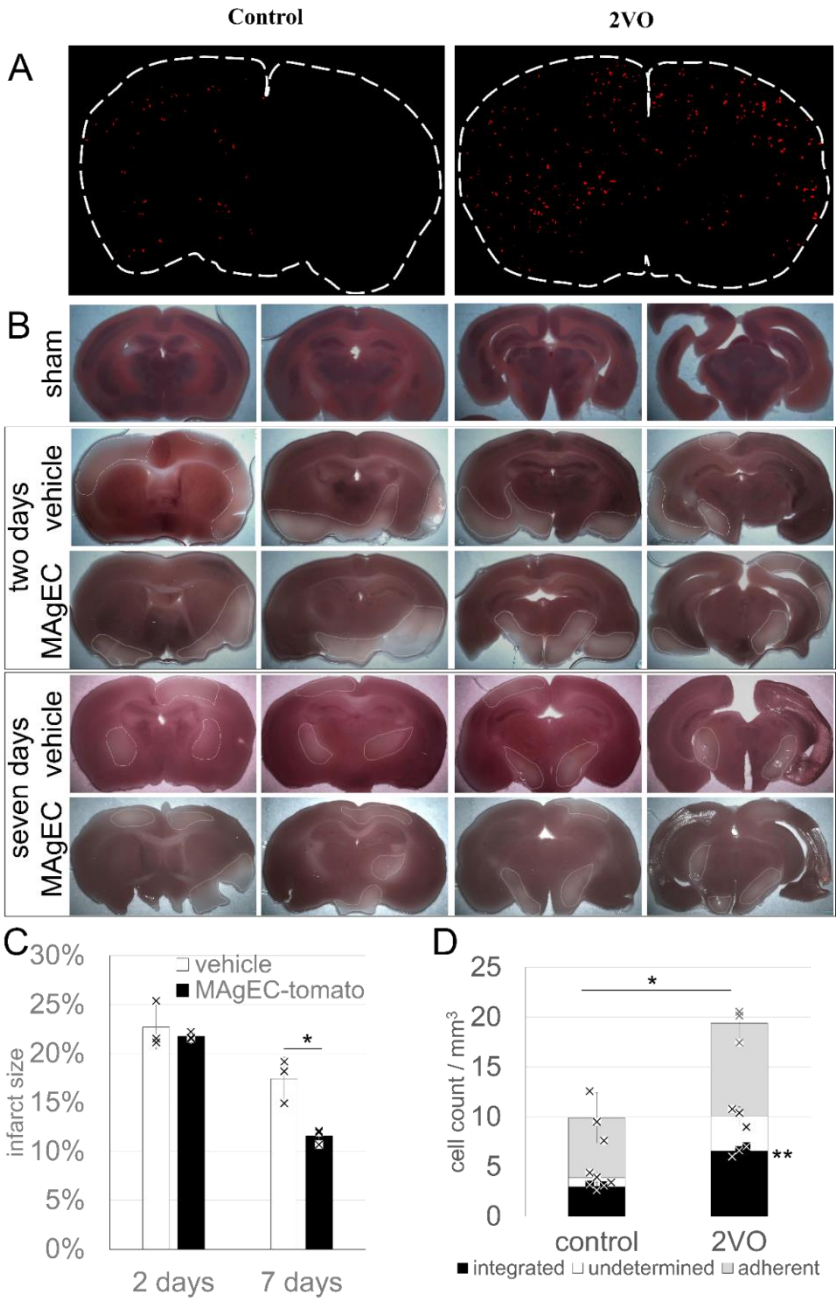

Figure 14. Effects of experimental hypoxia on EPC adhesion and integration

A The initial ipsilateral distribution of EPC cells in healthy brains shifted to a uniform distribution across both hemispheres in hypoxia. Images were thresholded and contrasted for better visibility. **B** Representative image of TTC staining for infarct volume. The stained area (red) is the non-infarct area; while the unstained area (white) is the infarct area. **C** Summarized data showing the infarct volume (percentage of brain section) in treatment groups following 2VO ischemic stroke. n=3, t-test: * p = 0.013. **D** Both the number of adherent and integrated MAgEC 10.5-tomato increased in 2VO animals compared to controls 5 days after injection. n=3, 16 sections each, t-test: ** p=0.00782 Bar graphs are means +- standard deviation.

5.7 Effect of senolysis on the adhesion and integration of EPCs *in vivo*

Using senolytic treatments on young and old BALB/c mice, we aimed to increase the number of EPC adhesion events by creating a niche for adhesion in place of the eliminated senescent endothelial cells. Mice underwent senolysis, then MAgEC 10.5-tomato injection, and 24 or 48 hours later, the number of adherent cells was counted (Figure 15A). We found that both senolytic treatments increased MAgEC 10.5-tomato adhesion to brain vasculature at both time points in young mice and after 48 hours in old mice (Figure 15B). The dasatinib + quercetin treatment caused a noticeably larger increase compared to abt-263. In old animals, there was a marked decrease in the number of adherent cells compared to young animals. 24 hours after injection, young animals had over 100 MAgEC 10.5-tomato cells per mm3 brain tissue while old animals had half as much. 48 hours after injection, the number of adherent cells in young animals was 63+/-4, while in old animals it was 30+/-5. Senolytic treatments were unable to completely negate the lower adhesion in old mice, even though the relative increase (compared to their respective controls) the senolytic treatments caused was similar. At 48 hours young animals had 109+/-5 or 140+/-11 adherent cells after abt-263 or dasatinib + quercetin (D+Q) pre-treatment while old ones had 42+/-8 and 53+/-8, respectively. The relative numbers of the effect of senolysis on EPC adhesion were only slightly less for old mice compared to young mice: 174%, 224% effect for abt-263 and D+Q in young animals while 140%, 176% in old animals (Figure 15C). As the integration of the EPCs into the vasculature took five days, we tested the effect of senolytic treatment on MAgEC 10.5-tomato integration in old BALB/c mice at this time point. Even though the groups for this experiment were smaller, we found a significant increase in dasatinib + quercetin pretreated animals (Figure 15D). Lastly, we checked whether MAgEC 10.5-tomato cells reached other organs besides the brain after intracarotid injection, and found deficient cells counts after two days (Figure 15E) and none after five days (not shown).

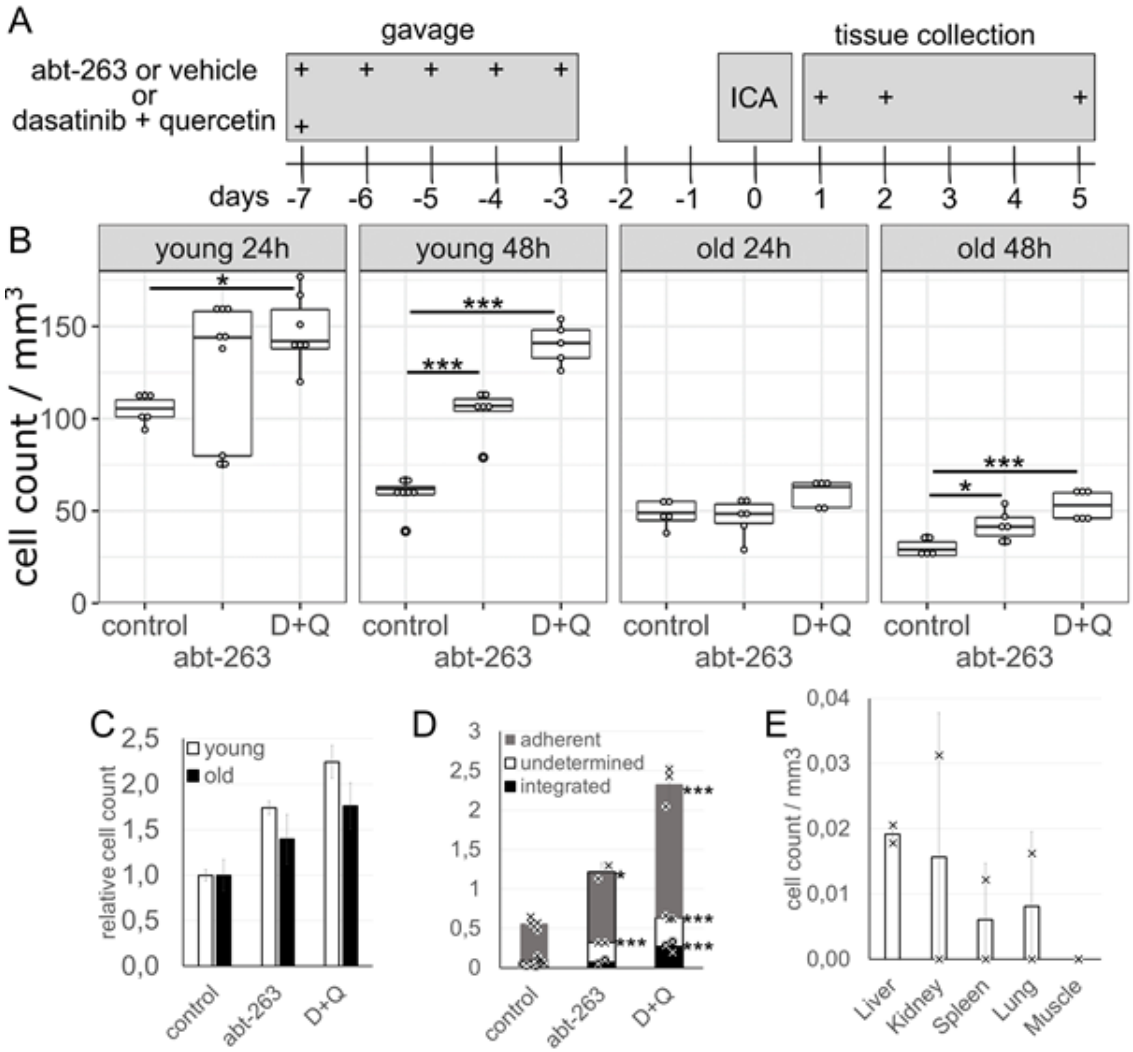

Figure 15. Effect of senolysis on EPC adhesion and integration *in vivo*

A Treatment schedule for senolytics and progenitor injections. Young and old BALB/c mice were pre-treated with either abt-263 or dasatinib + quercetin (D+Q). A week later MAgEC 10.5-tomato cells were injected through the internal carotid artery. Brains were sectioned 24, 48 hours, or 5 days after injection. **B** Adherent progenitor cells were counted on vibratome sections. The cell counts are presented as box plots. **C** Comparing the relative effect of senolysis on 48-hour progenitor cell adhesion between young and old mice by normalizing to the adherent cell numbers of the respective controls (comparing 2nd and 4th panels of B). **D** MAgEC 10.5-tomato cells adhesion and integration in old mice 5 days after injections and in response to senolytic treatment. Control n=4, abt-263 n=2, D+Q n=3. **E** In young mice, 48 hours after intracarotid injection, there were negligible numbers of adherent MAgECs in the liver, kidney, spleen, lung, and muscle tissue (n=2). Significance values are based on ANOVA. * $p \leq 0.05$, *** $p \leq 0.01$ Bar graphs are means +- standard deviation. All data points belong to individual animals and were presented in each graph.

6. DISCUSSION

The well-being of the brain is crucial for maintaining good health and promoting longevity. Older individuals suffering from age-related neurovascular and neurodegenerative diseases often experience dysfunction of the capillary vessel endothelium, leading to impaired neurovascular unit function.

Since 1997, when Asahara and colleagues sparked the study of endothelial progenitor cells, it is clear that EPCs have therapeutic potential. EPCs home in on hypoxic signals and have tissue regenerative properties. These two attributes opened the way for some obvious and less obvious therapeutic strategies. Considering that more than two decades passed, it is surprising that very little is known about the adhesion and integration dynamics of EPCs to the brain vasculature.

Thus we started our studies by observing MAgEC 10.5 EPCs in the brain tissue of mice. To make the observation possible we made the cells fluorescent by chemical labelling. MAgEC 10.5 cells injected into the internal carotid artery quickly adhered to the capillaries of the ipsilateral hemisphere. Negligible numbers of MAgEC 10.5 cells were found in peripheral tissues supporting that EPCs adhered to blood vessels shortly after injection and did not pass through the circulation multiple times. As hypoxia increases the adhesion of EPCs to mature endothelium, this unilateral distribution could be at least partially explained by a short and slight hypoxia caused by the injection in the ipsilateral internal carotid, or the injected cells themselves can cause hypoperfusion in their vicinity, as shown before (Cui et al., 2015). Ohta and colleagues also observed ipsilateral distribution of EPCs in Sprague-Dawley rats after causing hypoxic injury via middle cerebral artery occlusion (MCAO) (Ohta et al., 2006). The injected MAgEC 10.5 cells could be observed adherent to the vasculature for multiple days although with diminishing numbers over time. In *ex vivo* brain sections less than 5% of adherent MAgEC 10.5 were found at vessel bifurcations. *In vivo* approximately one in four MAgEC 10.5 were found adherent at capillary bifurcations. During the first two days after the injections MAgEC 10.5 was observed to fill but not completely block the lumen of capillaries. We seldom observed blood in brain vessels next to adherent MAgEC 10.5 *ex vivo* after transcardial perfusion or collapsed capillaries during intravital microscopy. Furthermore, intravital microscopy showed that fluorescent dyes injected into the bloodstream reached the capillary

segments past adherent MAgEC 10.5. In some cases we observed adherent MAgEC 10.5 cells flattened against the capillary wall already 28 hours after injection.

For longer studies of EPC interaction dynamics with the brain vasculature, MAgEC 10,5 cells were modified to express the red fluorescent protein tdTomato. In healthy BALB/c mouse brains, we observed that some of the fluorescent MAgEC 10.5-tomato cells integrated into the vasculature within five days. To our knowledge, we are the first to demonstrate that EPC-derived endothelial cells incorporated into microvessels next to pre-existing endothelial cells and displayed continuous TJs between these cells as indicated by claudin-5 immunolabelling. We also found that the number of MAgEC 10.5 cells observed in brain tissue decreased over time after injection. These MAgEC 10.5-derived, red fluorescent endothelial cells were observed in capillary vessels in the brain parenchyma, usually in small groups of 1-3 cells, but did not form large vascular trees of multiple MAgEC 10.5-derived cells.

To assess the dynamics of EPC-brain vasculature interactions we followed MAgEC 10.5-tomato cells in the brain of FVB/Ant:TgCAG-yfp_sb #27 mice by intravital two-photon microscopy. In a cranial window, we could image approximately 4-9 volumes of 700*700*400μm brain tissue. It was rare for EPC to stay at the same location for multiple days. In a five-day period, only around 3 cells out of 10 could be found again at the same location. TNFα levels are increased both in aging and in stroke (Bruunsgaard et al., 2008; Xue et al., 2022) and TNFα treatment increased both bond number and affinity between early outgrowth EPCs and rat cardiac microvascular endothelial cells (Prisco et al., 2015). Thus, we tested the effect of TNFα pre-treatment in our *in vivo* system and found that the number of EPCs adherent to the cortical microvasculature nearly doubled and most of the pre-treated cells stayed adherent to the same location for five days. Chronic exposure to TNFα causes senescence in EPCs (Y. Zhang et al., 2009), thus we used a short and low-concentration TNFα treatment to minimize chronic effects.

We theorized, that EPCs interacting with the brain vasculature could affect blood-brain barrier function. To test this, we used the two classical fluorescent tracers: Evans blue and Na-fluorescein as transcellular or paracellular permeability tracers respectively. The fluorescent signal of the tracers was monitored intravitally using two-photon microscopy capillaries that contained MAgEC-tomato cells, however, we detected no significant changes compared to control vessels.

As MAgEC 10.5 cells can spend several days adhered to brain vasculature, it follows that these cells could be used for the local delivery of therapeutic substances. To explore this idea we injected MAgEC 10.5 cells that secrete active antibody fragments. Our collaborating partners developed two MAgEC 10.5 daughter cell lines for testing the therapeutic potential of expressing fragment antigen binding regions or Fab-s in the central nervous system (Thinard et al., 2022). Our results demonstrated the localization of anti-TDP43 Fabs in the perivascular space and the brain parenchyma. Immunostaining of astrocyte end-feet, using aquaporin-4 as a specific marker, revealed a clear presence of Fabs in the brain parenchyma, past the aquaporin signal. These findings suggest that genetically modified EPCs could be used to introduce antibodies or other therapeutic proteins into the brain parenchyma. Our collaboration partners demonstrated that these anti-TDP43 Fabs can bind to TDP-43 aggregates, solubilizing a significant fraction of them in a concentration-dependent manner making our *in vivo* results a basic proof-of-concept for *in vivo* cell-gene therapy for neurodegenerative disease treatment. This supports the potential to expand the treatment strategy by applying it to ALS-diseased mice in future studies. For instance, it is assumed that mice with the SOD1 mutation might develop the required conditions, such as a hypoxic BBB, along with the production of TDP-43 in the brain parenchyma, allowing for long-term assessment of post-treatment movement recovery in animals (Joyce et al., 2015). During these experiments, we observed red fluorescent capillary vessel sections in the brain suggesting that EPCs can differentiate into brain endothelial cells and integrate into the brain capillary bed. Successful immunofluorescence staining of the tight junction protein claudin-5 supported this. The neurodegeneration therapy method presented above enhances existing therapeutic applications of EPCs (Collet et al., 2016; Garbuzova-Davis et al., 2008; Heller et al., 2020) by using transfected EPCs that express active antibody fragments or therapeutic proteins (Collet et al., 2016). The use of MAgEC 10.5 cells expressing anti-TDP-43 Fabs has two key aspects. First, the EPCs themselves help repair the damaged BBB observed in ALS and AD models. Second, the transfected EPCs secrete therapeutic agents at the BBB, which have the potential to solubilize TDP43 aggregates.

The literature regarding the roles of EPCs in the brain mainly focuses on tissue-level regeneration following ischemic injury and largely disregards localization and subsequent fate of injected EPCs in the brain. Contrasting our finding that embryonic EPCs integrate into microvessels in healthy mice, two groups reported that under ischemic conditions in rats, EPCs differentiated into brain endothelial cells in larger blood vessels. The first mention of EPCs

integrating into brain vasculature that we found is from 2002 where Zhang et al. injected bone marrow cells from Tie2-LacZ mice in the tail vein of FVB mice that underwent MCAO. They could detect newly differentiated Xgal-positive endothelial cells at the infarct border in 20-50 μm vessels 30 days after ischemia (Z. G. Zhang et al., 2002). Similarly, in Sprague Dawley rats that underwent hypoxia/reperfusion in a 3-vessel occlusion model, CD34+ peripheral blood cells were found to integrate into the walls of 100 μm diameter vessels in the penumbra after 28 days (Shyu et al., 2006). Data available that show EPCs at microvessels focus on EPC localization in the ischemic area but do not examine the integration of EPCs. In CD-1 mice, Fan et al. observed that Dil-labelled EPCs – cultured from human blood – injected through the jugular vein resided in the hypoxic zone at microvessels 24 hours after MCAO (Fan et al., 2010). In male C57BL/6 mice that underwent permanent MCAO, BrdU-labelled EPCs derived from bone marrow were observed at microvessel walls 3 days after injection in the ischemic area (Xin et al., 2016). As literature data is mainly concentrated on neuron survival and the vascularisation of post-ischemic tissue, we studied EPC integration in the 2VO model using our model EPC line to show that it acts similar to the cell types used by others - in that it alleviates detrimental effects after ischemic injury in the brain. Our results showed significantly decreased tissue damage based on TTC staining in mice injected with MAgEC 10.5-tomato cells after ischemic injury. Interestingly, the ipsilateral distribution of MAgEC 10.5-tomato cells observed in healthy brains shifted to a uniform distribution in both hemispheres after 2VO. At the same time, the number of MAgEC 10.5-tomato in brain tissue and more importantly the number of integrated EPCs was significantly increased. The higher number of EPC adhesion and integration into the microvasculature is in good agreement with the observed increase in tissue healing.

Since senolysis clears senescent cells from tissues, we theorized that this can promote the adhesion of EPCs in circulation in place of the removed senescent cells. Thus we injected the red fluorescent MAgEC 10.5-tomato cells into mice that were pretreated using senolytics. Combining senolysis and EPC therapy, we demonstrated that both abt-263 and the combination of dasatinib with quercetin significantly increased the number of MAgEC 10.5-tomato cells interacting with the vasculature both in young and old mice. The effect was slower to develop in old mice and as the adherent cell counts were already lower, the senotherapy-induced increase appeared low. However, the relative effect of senolysis was similar in old and young mice. Furthermore, we showed that both senolytic treatments increased the number of

integrated MAgEC 10.5-tomato in old mice. While the finding that EPCs adhere to old vasculature in lower numbers might seem counterintuitive as a more damaged, old endothelium was expected to recruit more EPCs, similar results have been reported in a skin hypoxia model. There the authors explained the observation by decreased hypoxic response of the affected tissue rather than decreased EPC mobilization or function (E. I. Chang et al., 2007). The idea that it is not EPC mobilization that is affected by aging is supported by the increased number of EPCs in older humans who have higher cerebral small vessel disease scores (Kapoor et al., 2021b).

In conclusion, by studying MAgEC 10.5 early embryonic EPCs *in vivo* and *ex vivo* in the mouse brain we described EPC-brain vasculature interaction dynamics including the integration of MAgEC 10.5 cells into the vascular bed. Genetically modified MAgEC 10.5 cells adherent to the brain vasculature were able to produce therapeutic Fabs that appeared inside the brain parenchyma suggesting that the use of genetically modified EPCs is a useful platform for the production of therapeutic proteins at the place of their action. Comparing EPC interaction dynamics in young and old mice, we found that endothelial progenitor cells adhered less to old brain vasculature, which was counteracted by combining EPC injections with senolytic therapy. The interaction of EPCs was also increased when the EPCs were activated beforehand. A promising candidate for this is TNFα, as it increased both the number of adherent cells and the time the cells remained adherent at the same location *in vivo*. Furthermore, we demonstrated increased adhesion and integration of EPCs in response to ischemic injury that may form the basis of the regenerative potential of EPC-based treatment.

Further studies are needed to test whether senolysis-amplified EPC adhesion and integration leads to improved tissue vascularisation and decreased cognitive deficit in aging. Our results also warrant further studies using these combined therapies in the manifold pathologies where EPCs or senolysis were found effective such as neurodegenerative diseases (Custodia et al., 2022b; Lee et al., 2021) and age-related pathologies where animal models are available (Hainsworth et al., 2017).

7. SUMMARY

Nowadays, aging poses a growing challenge to the society and economy of developed countries. Aging is a series of physiological processes that are generally unavoidable. However, the aging population compels society to confront the rising prevalence of ischemic stroke and neurodegenerative diseases.

Cerebral blood flow (CBF) is vital for normal brain function, delivering oxygen and glucose to neurons. Local CBF is regulated by the neurovascular unit (NVU) through a process known as neurovascular coupling, a specialized mechanism unique to mammals. The NVU comprises several cellular components: neurons, perivascular astrocytes, pericytes, microglia, and endothelial cells. The aging process leads to structural and functional impairments in the NVU. Aging reduces the capillary density within the brain capillary network, compromising its ability to sustain adequate CBF. Additionally, with aging, the number of senescent cells increases which induces tissue damage through increased inflammation. Senescence is a defense mechanism against tumor development since it prevents the replication of cells with damaged genomes; however, as senescence cells accumulate, it can become pathologic.

Since 1997, the pioneering work of Asahara and colleagues has ignited interest in the study of endothelial progenitor cells (EPCs). EPCs, along with local endothelial cells in vessel walls, have the potential to repair blood vessel damage making EPCs a promising candidate for cell-based therapies. However, relatively little is known about the adhesion and integration dynamics of EPCs within the brain vasculature. This study focuses on EPC interactions with brain vasculature under physiological conditions, during aging, and after ischemic injury. A key objective was to explore a novel approach involving the *ex vivo* transfection of EPCs to serve as cellular producers of antibody fragments targeting misfolded proteins associated with neurodegenerative diseases. Another key goal was to improve the efficacy of EPC therapy. To this end we eliminated senescent cells using senolytics to potentially make room for more EPC integration. Another avenue we explored was to increase the cell adhesive properties of EPCs by activating them before injection.

We utilized an immortalized cell line derived from embryonic mouse aorta–gonad–mesonephros endothelial cells (MAgEC 10.5). To enable *in vivo* tracking during long-term experiments, MAgEC 10.5 cells were transduced to express the red fluorescent protein tdTomato, this daughter cell line was named MAgEC 10.5-tomato. Additionally, MAgEC 10.5

cells were modified to express anti-TDP-43 Fabs to investigate their potential as a vector for local expression of therapeutic molecules in the diseased tissue. We employed intravital two-photon microscopy to monitor fluorescently labeled MAgEC 10.5 *in vivo* and immunohistochemistry combined with laser scanning microscopy to analyze the behavior of these cells *ex vivo*.

Fluorescent MAgEC 10.5 EPCs were injected into the common carotid artery of BALB/c mice. After injections, the brains were sectioned at various time points. We observed that most MAgEC 10.5 completely filled the capillary lumen in brain sections after injection. Later, some EPCs were flattened against and stuck to vessel walls. After about five days we observed a few MAgEC 10.5 cells integrated into brain capillaries. We were the first to show that EPCs adherent to the brain vasculature integrated into microvessels and took up endothelial morphology, established tight junctions, and formed vessel lumens together with neighboring endothelial cells. Injected MAgEC 10.5 were almost exclusively detected in the hemisphere ipsilateral to the injection, suggesting that EPCs adhered to the vasculature shortly after injection and did not pass through the circulation multiple times. Early adhesion of EPCs in brain vessels after intracarotid injection was further supported by our finding of meager numbers of MAgEC 10.5 cells in peripheral tissues.

To assess the dynamics of EPC-brain vasculature interactions for longer studies, we followed MAgEC 10.5-tomato cells in the brain of FVB/Ant: TgCAG-yfp sb #27 mice that express the Venus yellow fluorescent protein in endothelial cells by intravital two-photon microscopy. It was rare for MAgEC 10.5-tomato cells to stay at the same location for multiple days unless the cells were activated previously by TNFα. TNFα not only increased the number of adherent cells but also prolonged their adhesion at the same location. We also showed that the arrest of EPCs induced no changes in blood-brain barrier function, based on *in vivo* permeability assays using intravital two-photon microscopy with classical fluorescent tracers.

Since MAgEC 10.5 cells can remain attached to brain vasculature for several days, they may serve as a means for local delivery of therapeutic agents. Our collaborators created MAgEC 10.5 derivative cell lines that release therapeutic fragment antigen-binding regions or Fabs. They showed that the Fabs secreted by these cells can solubilize the neurotoxic β-amyloid or TDP-43 protein aggregates *in vitro*. To evaluate whether this system can be used to introduce the therapeutic Fabs into the central nervous system. Our results showed that MAgEC 10.5 cells expressing anti-TDP-43 Fabs retained the transgene expression after adhering to the brain

vasculature *in vivo*. Most of the secreted Fab is localized at the vessel wall, but some could be detected in the brain parenchyma as well. These results demonstrate that antibodies secreted at the brain vasculature by transgenic EPCs can successfully penetrate into the brain parenchyma. The use of MAgEC 10.5 cells expressing anti-TDP-43 Fabs has two key aspects. First, the EPCs themselves help repair the damaged vasculature. Second, the cells secreted the therapeutic Fab at the site of therapy and introduced it into the brain parenchyma where it could help treat ALS by solubilizing TDP-43 aggregates.

We investigated the integration of MAgEC 10.5-tomato cells using the 2VO model, employing the MAgEC 10.5-tomato cell line to show that it acts similar to the cell types used by others - in that it alleviates detrimental effects after ischemic injury and to study whether the integration of these cells could play a role in this. Our findings revealed significant tissue regeneration in mice injected with MAgEC 10.5-tomato cells following ischemic damage. Concurrently, the number of MAgEC 10.5-tomato cells in brain tissue and, more importantly, the number of integrated MAgEC 10.5-tomato cells, was significantly increased.

Since senolysis eliminates senescent cells from tissues, we hypothesized that this process could enhance the adhesion of circulating EPCs by making space with the removal of the senescent cells. To test this hypothesis, we injected red fluorescent MAgEC 10.5-tomato cells into mice pretreated with senolytics. We found that the two senolytic treatments we used, Abt-263 and the dasatinib-quercetin combination both significantly increased the interaction of MAgEC 10.5-tomato cells with the vasculature in both young and old mice. Furthermore, we demonstrated that both senolytic treatments enhanced the integration of MAgEC 10.5-tomato cells in old mice.

In conclusion, EPCs rapidly adhere to the vasculature following injection. We demonstrated that EPCs integrate into microvessels and contribute to vessel formation, underscoring their efficacy in promoting brain tissue healing after injury. Pre-activation of EPCs enhanced their interaction with the vasculature. TNFα emerged as a promising candidate for this purpose. Genetically modified EPCs can be used as a platform to introduce therapeutic Fabs directly into the brain parenchyma. EPCs adhered less to old brain vasculature compared to young brains, which was counteracted by combining EPC injections with senolytic therapy. Furthermore, we demonstrated not only increased adhesion but also increased integration of EPCs in response to ischemic injury that may form the basis of the regenerative potential of EPC-based treatment. Thus our study highlights the therapeutic potential of injected EPCs in

the brain vasculature which can be further enhanced using senolytics, EPC activation, and genetic modification of EPCs.

8. ACKNOWLEDGEMENTS

As I write this PhD thesis, I am overwhelmed with emotion and excitement, knowing that I am nearing a significant milestone in my life: completing my doctoral degree. Over the past four years, my beautiful journey in Szeged, Hungary has been filled with countless unforgettable experiences, encompassing both joy and challenges. On this occasion, I would like to express my deepest gratitude to everyone who, in any way, contributed to the successful completion of this thesis.

First and foremost, my deepest gratitude goes to my main supervisor, Dr. Attila Elek Farkas, for offering me this PhD position and making me a part of the Doctoral School of Biology at the University of Szeged. His passion and dedication to scientific research have been a profound source of inspiration throughout my four-year PhD journey and my future career. I am especially grateful for his ability to clarify complex concepts through effective communication and for the invaluable opportunity to learn from his extensive expertise and knowledge in the field. It has been an incredible experience to gain so much from him over the years, and I continue to learn even now. Thank you for everything—I am truly proud to be his student. I would also like to sincerely thank Prof. Dr. István A. Krizbai, head of the Neurovascular Unit group, and Dr. Imola Wilhelm for their important discussions and unwavering support.

A special thanks go to all my beloved labmates - Dr. Csilla, Dr. Kinga, Dr.Ádám, Dr. Monika, Tamás, Fanni, Tejal, Mariam, Valentina, Isti, and all the members of the Neurovascular Unit group - for their invaluable contributions to scientific discussions, troubleshooting, and communication in the laboratory. I will never forget our laughter-filled lunch breaks and the times we spent hanging out and enjoying drinks together, which helped create the perfect “work-life balance.” Each of you has been an indispensable part of my PhD journey.

I would like to thank the HUN-REN Biological Research Centre, Szeged, for providing me with an excellent research environment. I also extend my gratitude to all the teachers, staff, and both international and Hungarian PhD students in the department for their friendliness, kindness, and support.

I would also like to express my gratitude to the Tempus Public Foundation (TPF) – Stipendium Hungaricum scholarship for funding my PhD studies, making this incredible

opportunity possible, which would have otherwise been out of reach. would like to express my gratitude to Nguyen Tat Thanh University and the Department of Science and Technology for nominating me to participate in this program. I also extend my heartfelt thanks to my colleagues for their kind words and encouragement throughout my study period.

Last but not least, my heartfelt thanks go to my family for their unconditional love and support. Your wisdom, kindness, and encouragement have always inspired me to strive for better. You have continuously motivated me to explore new horizons and have stood by my side as I worked towards building a brighter future.

Thank you once again to all of you for shaping this improved version of myself. I look forward to stepping into a new milestone and carrying all these beautiful memories with me.

9. REFERENCES

Ahire, C., Nyul-Toth, A., DelFavero, J., Gulej, R., Faakye, J. A., Tarantini, S., Kiss, T., Kuan-Celarier, A., Balasubramanian, P., Ungvari, A., Tarantini, A., Nagaraja, R., Yan, F., Tang, Q., Mukli, P., Csipo, T., Yabluchanskiy, A., Campisi, J., Ungvari, Z., & Csiszar, A. (2023). Accelerated cerebromicrovascular senescence contributes to cognitive decline in a mouse model of paclitaxel (Taxol)-induced chemobrain. *Aging Cell*, *22*(7), e13832. https://doi.org/10.1111/acel.13832

Alexander, G. E., Ryan, L., Bowers, D., Foster, T. C., Bizon, J. L., Geldmacher, D. S., & Glisky, E. L. (2012). Characterizing cognitive aging in humans with links to animal models. *Frontiers in Aging Neuroscience*, *4*. https://doi.org/10.3389/fnagi.2012.00021

Aquino, J. B., Sierra, R., & Montaldo, L. A. (2021). Diverse cellular origins of adult blood vascular endothelial cells. *Developmental Biology*, *477*, 117–132. https://doi.org/10.1016/j.ydbio.2021.05.010

Asahara, T., Murohara, T., Sullivan, A., Silver, M., Van Der Zee, R., Li, T., Witzenbichler, B., Schatteman, G., & Isner, J. M. (1997). Isolation of Putative Progenitor Endothelial Cells for Angiogenesis. *Science*, *275*(5302), 964–966. https://doi.org/10.1126/science.275.5302.964

Atik, A., Stewart, T., & Zhang, J. (2016). Alpha-Synuclein as a Biomarker for Parkinson's Disease. *Brain Pathology*, *26*(3), 410–418. https://doi.org/10.1111/bpa.12370

Azam, S., Haque, Md. E., Balakrishnan, R., Kim, I.-S., & Choi, D.-K. (2021). The Ageing Brain: Molecular and Cellular Basis of Neurodegeneration. *Frontiers in Cell and Developmental Biology*, *9*, 683459. https://doi.org/10.3389/fcell.2021.683459

Baker, D. J., Wijshake, T., Tchkonia, T., LeBrasseur, N. K., Childs, B. G., Van De Sluis, B., Kirkland, J. L., & Van Deursen, J. M. (2011). Clearance of p16Ink4a-positive senescent cells delays ageing-associated disorders. *Nature*, *479*(7372), 232–236. https://doi.org/10.1038/nature10600

Banerjee, S., Bentley, P., Hamady, M., Marley, S., Davis, J., Shlebak, A., Nicholls, J., Williamson, D. A., Jensen, S. L., Gordon, M., Habib, N., & Chataway, J. (2014). Intra-Arterial Immunoselected CD34+ Stem Cells for Acute Ischemic Stroke. *Stem Cells Translational Medicine*, *3*(11), 1322–1330. https://doi.org/10.5966/sctm.2013-0178

Bautch, V. L., & Caron, K. M. (2015). Blood and lymphatic vessel formation. *Cold Spring Harbor Perspectives in Biology*, *7*(3), a008268. https://doi.org/10.1101/cshperspect.a008268

Béjot, Y., Bailly, H., Durier, J., & Giroud, M. (2016). Epidemiology of stroke in Europe and trends for the 21st century. *La Presse Médicale*, *45*(12), e391–e398. https://doi.org/10.1016/j.lpm.2016.10.003

Braak, H., Brettschneider, J., Ludolph, A. C., Lee, V. M., Trojanowski, J. Q., & Tredici, K. D. (2013). Amyotrophic lateral sclerosis—A model of corticofugal axonal spread. *Nature Reviews Neurology*, *9*(12), 708–714. https://doi.org/10.1038/nrneurol.2013.221

Brown, W. R., & Thore, C. R. (2011). Review: Cerebral microvascular pathology in ageing and neurodegeneration. *Neuropathology and Applied Neurobiology*, *37*(1), 56–74. https://doi.org/10.1111/j.1365-2990.2010.01139.x

Bruning, A. (2013). Inhibition of mTOR Signaling by Quercetin in Cancer Treatment and Prevention. *Anti-Cancer Agents in Medicinal Chemistry*, *13*(7), 1025–1031. https://doi.org/10.2174/18715206113139990114

Bruunsgaard, H., Skinhøj, P., Pedersen, A. N., Schroll, M., & Pedersen, B. K. (2008). Ageing, tumour necrosis factor-alpha (TNF- α) and atherosclerosis. *Clinical and Experimental Immunology*, *121*(2), 255–260. https://doi.org/10.1046/j.1365-2249.2000.01281.x

Burton, D. G. A., & Krizhanovsky, V. (2014). Physiological and pathological consequences of cellular senescence. *Cellular and Molecular Life Sciences*, *71*(22), 4373–4386. https://doi.org/10.1007/s00018-014-1691-3

Bussian, T. J., Aziz, A., Meyer, C. F., Swenson, B. L., Van Deursen, J. M., & Baker, D. J. (2018). Clearance of senescent glial cells prevents tau-dependent pathology and cognitive decline. *Nature*, *562*(7728), 578–582. https://doi.org/10.1038/s41586-018-0543-y

Carracedo, J., Ramírez-Carracedo, R., Alique, M., & Ramírez-Chamond, R. (2018). Endothelial Cell Senescence in the Pathogenesis of Endothelial Dysfunction. In H. Lenasi (Ed.), *Endothelial Dysfunction—Old Concepts and New Challenges*. InTech. https://doi.org/10.5772/intechopen.73024

Chaib, S., Tchkonia, T., & Kirkland, J. L. (2022). Cellular senescence and senolytics: The path to the clinic. *Nature Medicine*, *28*(8), 1556–1568. https://doi.org/10.1038/s41591-022-01923-y

Chang, E. I., Loh, S. A., Ceradini, D. J., Chang, E. I., Lin, S., Bastidas, N., Aarabi, S., Chan, D. A., Freedman, M. L., Giaccia, A. J., & Gurtner, G. C. (2007). Age Decreases Endothelial Progenitor Cell Recruitment Through Decreases in Hypoxia-Inducible Factor 1α Stabilization During Ischemia. *Circulation*, *116*(24), 2818–2829. https://doi.org/10.1161/CIRCULATIONAHA.107.715847

Chang, J., Wang, Y., Shao, L., Laberge, R.-M., Demaria, M., Campisi, J., Janakiraman, K., Sharpless, N. E., Ding, S., Feng, W., Luo, Y., Wang, X., Aykin-Burns, N., Krager, K., Ponnappan, U., Hauer-Jensen, M., Meng, A., & Zhou, D. (2016). Clearance of senescent cells by ABT263 rejuvenates aged hematopoietic stem cells in mice. *Nature Medicine*, *22*(1), 78–83. https://doi.org/10.1038/nm.4010

Chen, K., Li, Y., Xu, L., Qian, Y., Liu, N., Zhou, C., Liu, J., Zhou, L., Xu, Z., Jia, R., & Ge, Y.-Z. (2022). Comprehensive insight into endothelial progenitor cell-derived extracellular vesicles as a promising candidate for disease treatment. *Stem Cell Research & Therapy*, *13*(1), 238. https://doi.org/10.1186/s13287-022-02921-0

Cheng, Y.-W., Yang, L.-Y., Chen, Y.-T., Chou, S.-C., Chen, K.-W., Chen, Y.-H., Deng, C.-R., Chen, I.-C., Chou, W.-J., Chang, C.-C., Chen, Y.-R., Hwa, H.-L., Wang, K.-C., & Kuo, M.-F. (2023). *EPCs-derived conditioned medium mitigates chronic cerebral ischemic injury through the MIF-activated AKT pathway*. Neurology. https://doi.org/10.1101/2023.11.19.23298748

Childs, B. G., Baker, D. J., Wijshake, T., Conover, C. A., Campisi, J., & Van Deursen, J. M. (2016). Senescent intimal foam cells are deleterious at all stages of atherosclerosis. *Science*, *354*(6311), 472–477. https://doi.org/10.1126/science.aaf6659

Collet, G., Szade, K., Nowak, W., Klimkiewicz, K., El Hafny-Rahbi, B., Szczepanek, K., Sugiyama, D., Weglarczyk, K., Foucault-Collet, A., Guichard, A., Mazan, A., Nadim, M., Fasani, F., Lamerant-Fayel, N., Grillon, C., Petoud, S., Beloeil, J.-C., Jozkowicz, A., Dulak, J., & Kieda, C. (2016). Endothelial precursor cell-based therapy to target the pathologic angiogenesis and compensate tumor hypoxia. *Cancer Letters*, *370*(2), 345–357. https://doi.org/10.1016/j.canlet.2015.11.008

Costea, L., Mészáros, Á., Bauer, H., Bauer, H.-C., Traweger, A., Wilhelm, I., Farkas, A. E., & Krizbai, I. A. (2019). The Blood-Brain Barrier and Its Intercellular Junctions in Age-Related Brain Disorders. *International Journal of Molecular Sciences*, *20*(21). https://doi.org/10.3390/ijms20215472

Cui, L., Kerkelä, E., Bakreen, A., Nitzsche, F., Andrzejewska, A., Nowakowski, A., Janowski, M., Walczak, P., Boltze, J., Lukomska, B., & Jolkkonen, J. (2015). The cerebral embolism evoked by intra-arterial delivery of allogeneic bone marrow mesenchymal stem cells in rats is related to cell dose and infusion velocity. *Stem Cell Research & Therapy*, *6*(1), 11. https://doi.org/10.1186/scrt544

Custodia, A., Ouro, A., Sargento-Freitas, J., Aramburu-Núñez, M., Pías-Peleteiro, J. M., Hervella, P., Rosell, A., Ferreira, L., Castillo, J., Romaus-Sanjurjo, D., & Sobrino, T. (2022a). Unraveling the potential of endothelial progenitor cells as a treatment following ischemic stroke. *Frontiers in Neurology*, *13*, 940682. https://doi.org/10.3389/fneur.2022.940682

Custodia, A., Ouro, A., Sargento-Freitas, J., Aramburu-Núñez, M., Pías-Peleteiro, J. M., Hervella, P., Rosell, A., Ferreira, L., Castillo, J., Romaus-Sanjurjo, D., & Sobrino, T. (2022b). Unraveling the potential of endothelial progenitor cells as a treatment following ischemic stroke. *Frontiers in Neurology*, *13*, 940682. https://doi.org/10.3389/fneur.2022.940682

D. Edelstein, A., A. Tsuchida, M., Amodaj, N., Pinkard, H., D. Vale, R., & Stuurman, N. (2014). Advanced methods of microscope control using μManager software. *Journal of Biological Methods*, *1*(2), 1. https://doi.org/10.14440/jbm.2014.36

Desjardins, M., Berti, R., Lefebvre, J., Dubeau, S., & Lesage, F. (2014). Aging-related differences in cerebral capillary blood flow in anesthetized rats. *Neurobiology of Aging*, *35*(8), 1947–1955. https://doi.org/10.1016/j.neurobiolaging.2014.01.136

Dudley, A. C., & Griffioen, A. W. (2023). The modes of angiogenesis: An updated perspective. *Angiogenesis*, *26*(4), 477–480. https://doi.org/10.1007/s10456-023-09895-4

Edelstein, A., Amodaj, N., Hoover, K., Vale, R., & Stuurman, N. (2010). Computer Control of Microscopes Using μManager. *Current Protocols in Molecular Biology*, *92*(1). https://doi.org/10.1002/0471142727.mb1420s92

Erusalimsky, J. D. (2009). Vascular endothelial senescence: From mechanisms to pathophysiology. *Journal of Applied Physiology*, *106*(1), 326–332. https://doi.org/10.1152/japplphysiol.91353.2008

Esquiva, G., Grayston, A., & Rosell, A. (2018). Revascularization and endothelial progenitor cells in stroke. *American Journal of Physiology-Cell Physiology*, *315*(5), C664–C674. https://doi.org/10.1152/ajpcell.00200.2018

Fan, Y., Shen, F., Frenzel, T., Zhu, W., Ye, J., Liu, J., Chen, Y., Su, H., Young, W. L., & Yang, G. (2010). Endothelial progenitor cell transplantation improves long-term stroke outcome in mice. *Annals of Neurology*, *67*(4), 488–497. https://doi.org/10.1002/ana.21919

Fang, J., Guo, Y., Tan, S., Li, Z., Xie, H., Chen, P., Wang, K., He, Z., He, P., Ke, Y., Jiang, X., & Chen, Z. (2019). Autologous Endothelial Progenitor Cells Transplantation for Acute Ischemic Stroke: A 4-Year Follow-Up Study. *Stem Cells Translational Medicine*, *8*(1), 14–21. https://doi.org/10.1002/sctm.18-0012

Fujisawa, T., Tura-Ceide, O., Hunter, A., Mitchell, A., Vesey, A., Medine, C., Gallogly, S., Hadoke, P. W. F., Keith, C., Sproul, A., Roddie, H., McQuaker, G., Wilmut, I., Mills, N. L., & Brittan, M. (2019). Endothelial Progenitor Cells Do Not Originate From the Bone Marrow. *Circulation*, *140*(18), 1524–1526. https://doi.org/10.1161/CIRCULATIONAHA.119.042351

Garbuzova-Davis, S., Saporta, S., & Sanberg, P. R. (2008). Implications of blood-brain barrier disruption in ALS. *Amyotrophic Lateral Sclerosis*, *9*(6), 375–376. https://doi.org/10.1080/17482960802160990

Geng, J., Wang, L., Qu, M., Song, Y., Lin, X., Chen, Y., Mamtilahun, M., Chen, S., Zhang, Z., Wang, Y., & Yang, G.-Y. (2017). Endothelial progenitor cells transplantation attenuated blood-brain barrier damage after ischemia in diabetic mice via HIF-1α. *Stem Cell Research & Therapy*, *8*(1), 163. https://doi.org/10.1186/s13287-017-0605-3

Gonzales, M. M., Garbarino, V. R., Kautz, T. F., Palavicini, J. P., Lopez-Cruzan, M., Dehkordi, S. K., Mathews, J. J., Zare, H., Xu, P., Zhang, B., Franklin, C., Habes, M., Craft, S., Petersen, R. C., Tchkonia, T., Kirkland, J. L., Salardini, A., Seshadri, S., Musi, N., & Orr, M. E. (2023). Senolytic therapy in mild Alzheimer's disease: A phase 1 feasibility trial. *Nature Medicine*, *29*(10), 2481–2488. https://doi.org/10.1038/s41591-023-02543-w

Hainsworth, A. H., Allan, S. M., Boltze, J., Cunningham, C., Farris, C., Head, E., Ihara, M., Isaacs, J. D., Kalaria, R. N., Lesnik Oberstein, S. A. M. J., Moss, M. B., Nitzsche, B., Rosenberg, G. A., Rutten, J. W., Salkovic-Petrisic, M., & Troen, A. M. (2017). Translational models for vascular cognitive impairment: A review including larger species. *BMC Medicine*, *15*(1), 16. https://doi.org/10.1186/s12916-017-0793-9

Haskó, J., Fazakas, C., Molnár, K., Mészáros, Á., Patai, R., Szabó, G., Erdélyi, F., Nyúl-Tóth, Á., Győri, F., Kozma, M., Farkas, A. E., Krizbai, I. A., & Wilhelm, I. (2019). Response of the neurovascular unit to brain metastatic breast cancer cells. *Acta Neuropathologica Communications*, *7*(1), 133. https://doi.org/10.1186/s40478-019-0788-1

Hatzopoulos, A. K., Folkman, J., Vasile, E., Eiselen, G. K., & Rosenberg, R. D. (1998). Isolation and characterization of endothelial progenitor cells from mouse embryos. *Development*, *125*(8), 1457–1468. https://doi.org/10.1242/dev.125.8.1457

Heller, L., Thinard, R., Chevalier, M., Arpag, S., Jing, Y., Greferath, R., Heller, R., & Nicolau, C. (2020). Secretion of proteins and antibody fragments from transiently transfected endothelial progenitor cells. *Journal of Cellular and Molecular Medicine*, *24*(15), 8772–8778. https://doi.org/10.1111/jcmm.15511

Huang, X., Li, M., Zhou, D., Deng, Z., Guo, J., & Huang, H. (2020). Endothelial progenitor cell transplantation restores vascular injury in mice after whole-brain irradiation. *Brain Research*, *1746*, 147005. https://doi.org/10.1016/j.brainres.2020.147005

Jo, M., Lee, S., Jeon, Y.-M., Kim, S., Kwon, Y., & Kim, H.-J. (2020). The role of TDP-43 propagation in neurodegenerative diseases: Integrating insights from clinical and experimental studies. *Experimental & Molecular Medicine*, *52*(10), 1652–1662. https://doi.org/10.1038/s12276-020-00513-7

Joyce, P. I., Mcgoldrick, P., Saccon, R. A., Weber, W., Fratta, P., West, S. J., Zhu, N., Carter, S., Phatak, V., Stewart, M., Simon, M., Kumar, S., Heise, I., Bros-Facer, V., Dick, J., Corrochano, S., Stanford, M. J., Luong, T. V., Nolan, P. M., … Acevedo-Arozena, A. (2015). A novel SOD1-ALS mutation separates central and peripheral effects of mutant SOD1 toxicity. *Human Molecular Genetics*, *24*(7), 1883–1897. https://doi.org/10.1093/hmg/ddu605

Kapoor, A., Gaubert, A., Marshall, A., Meier, I. B., Yew, B., Ho, J. K., Blanken, A. E., Dutt, S., Sible, I. J., Li, Y., Jang, J. Y., Brickman, A. M., Rodgers, K., & Nation, D. A. (2021a). Increased Levels of Circulating Angiogenic Cells and Signaling Proteins in Older Adults With Cerebral Small Vessel Disease. *Frontiers in Aging Neuroscience*, *13*, 711784. https://doi.org/10.3389/fnagi.2021.711784

Kapoor, A., Gaubert, A., Marshall, A., Meier, I. B., Yew, B., Ho, J. K., Blanken, A. E., Dutt, S., Sible, I. J., Li, Y., Jang, J. Y., Brickman, A. M., Rodgers, K., & Nation, D. A. (2021b). Increased Levels of Circulating Angiogenic Cells and Signaling Proteins in

Older Adults With Cerebral Small Vessel Disease. *Frontiers in Aging Neuroscience*, *13*, 711784. https://doi.org/10.3389/fnagi.2021.711784

Katsagoni, C. N., Kokkinos, P., & Sidossis, L. S. (2023). *Prevention and Management of Cardiovascular and Metabolic Disease: Diet, Physical Activity and Healthy Aging* (1st ed.). Wiley. https://doi.org/10.1002/9781119833475

Kesidou, E., Theotokis, P., Damianidou, O., Boziki, M., Konstantinidou, N., Taloumtzis, C., Sintila, S.-A., Grigoriadis, P., Evangelopoulos, M. E., Bakirtzis, C., & Simeonidou, C. (2023). CNS Ageing in Health and Neurodegenerative Disorders. *Journal of Clinical Medicine*, *12*(6), 2255. https://doi.org/10.3390/jcm12062255

Kirkland, J. L., & Tchkonia, T. (2020). Senolytic drugs: From discovery to translation. *Journal of Internal Medicine*, *288*(5), 518–536. https://doi.org/10.1111/joim.13141

Klimkiewicz, K., Weglarczyk, K., Collet, G., Paprocka, M., Guichard, A., Sarna, M., Jozkowicz, A., Dulak, J., Sarna, T., Grillon, C., & Kieda, C. (2017). A 3D model of tumour angiogenic microenvironment to monitor hypoxia effects on cell interactions and cancer stem cell selection. *Cancer Letters*, *396*, 10–20. https://doi.org/10.1016/j.canlet.2017.03.006

Kouhi, A., Pachipulusu, V., Kapenstein, T., Hu, P., Epstein, A. L., & Khawli, L. A. (2021). Brain Disposition of Antibody-Based Therapeutics: Dogma, Approaches and Perspectives. *International Journal of Molecular Sciences*, *22*(12), 6442. https://doi.org/10.3390/ijms22126442

Krzystyniak, A., Wesierska, M., Petrazzo, G., Gadecka, A., Dudkowska, M., Bielak-Zmijewska, A., Mosieniak, G., Figiel, I., Wlodarczyk, J., & Sikora, E. (2022). Combination of dasatinib and quercetin improves cognitive abilities in aged male Wistar rats, alleviates inflammation and changes hippocampal synaptic plasticity and histone H3 methylation profile. *Aging*, *14*(2), 572–595. https://doi.org/10.18632/aging.203835

Kuilman, T., Michaloglou, C., Mooi, W. J., & Peeper, D. S. (2010). The essence of senescence: Figure 1. *Genes & Development*, *24*(22), 2463–2479. https://doi.org/10.1101/gad.1971610

Kupatt, C., Hinkel, R., Lamparter, M., Von Brühl, M.-L., Pohl, T., Horstkotte, J., Beck, H., Müller, S., Delker, S., Gildehaus, F.-J., Büning, H., Hatzopoulos, A. K., & Boekstegers, P. (2005). Retroinfusion of Embryonic Endothelial Progenitor Cells Attenuates Ischemia-Reperfusion Injury in Pigs: Role of Phosphatidylinositol 3-Kinase/AKT

Kinase. *Circulation*, *112*(9_supplement). https://doi.org/10.1161/CIRCULATIONAHA.104.524801

Kupatt, C., Horstkotte, J., Vlastos, G. A., Pfosser, A., Lebherz, C., Semisch, M., Thalgott, M., Büttner, K., Browarzyk, C., Mages, J., Hoffmann, R., Deten, A., Lamparter, M., Müller, F., Beck, H., Büning, H., Boekstegers, P., & Hatzopoulos, A. K. (2005). Embryonic endothelial progenitor cells expressing a broad range of proangiogenic and remodeling factors enhance vascularization and tissue recovery in acute and chronic ischemia. *The FASEB Journal*, *19*(11), 1576–1578. https://doi.org/10.1096/fj.04-3282fje

Kwong, L. K., Irwin, D. J., Walker, A. K., Xu, Y., Riddle, D. M., Trojanowski, J. Q., & Lee, V. M. Y. (2014). Novel monoclonal antibodies to normal and pathologically altered human TDP-43 proteins. *Acta Neuropathologica Communications*, *2*(1), 33. https://doi.org/10.1186/2051-5960-2-33

Lee, S., Wang, E. Y., Steinberg, A. B., Walton, C. C., Chinta, S. J., & Andersen, J. K. (2021). A guide to senolytic intervention in neurodegenerative disease. *Mechanisms of Ageing and Development*, *200*, 111585. https://doi.org/10.1016/j.mad.2021.111585

Lu, Y., Jarrahi, A., Moore, N., Bartoli, M., Brann, D. W., Baban, B., & Dhandapani, K. M. (2023). Inflammaging, cellular senescence, and cognitive aging after traumatic brain injury. *Neurobiology of Disease*, *180*, 106090. https://doi.org/10.1016/j.nbd.2023.106090

Mattson, M. P., & Arumugam, T. V. (2018). Hallmarks of Brain Aging: Adaptive and Pathological Modification by Metabolic States. *Cell Metabolism*, *27*(6), 1176–1199. https://doi.org/10.1016/j.cmet.2018.05.011

Medina, R. J., Barber, C. L., Sabatier, F., Dignat-George, F., Melero-Martin, J. M., Khosrotehrani, K., Ohneda, O., Randi, A. M., Chan, J. K. Y., Yamaguchi, T., Van Hinsbergh, V. W. M., Yoder, M. C., & Stitt, A. W. (2017). Endothelial Progenitors: A Consensus Statement on Nomenclature. *Stem Cells Translational Medicine*, *6*(5), 1316–1320. https://doi.org/10.1002/sctm.16-0360

Melo Dos Santos, L., Trombetta-Lima, M., Eggen, B., & Demaria, M. (2024). Cellular senescence in brain aging and neurodegeneration. *Ageing Research Reviews*, *93*, 102141. https://doi.org/10.1016/j.arr.2023.102141

Moniche, F., Gonzalez, A., Gonzalez-Marcos, J.-R., Carmona, M., Piñero, P., Espigado, I., Garcia-Solis, D., Cayuela, A., Montaner, J., Boada, C., Rosell, A., Jimenez, M.-D.,

Mayol, A., & Gil-Peralta, A. (2012). Intra-Arterial Bone Marrow Mononuclear Cells in Ischemic Stroke: A Pilot Clinical Trial. *Stroke*, *43*(8), 2242–2244. https://doi.org/10.1161/STROKEAHA.112.659409

Montagne, A., Barnes, S. R., Sweeney, M. D., Halliday, M. R., Sagare, A. P., Zhao, Z., Toga, A. W., Jacobs, R. E., Liu, C. Y., Amezcua, L., Harrington, M. G., Chui, H. C., Law, M., & Zlokovic, B. V. (2015). Blood-Brain Barrier Breakdown in the Aging Human Hippocampus. *Neuron*, *85*(2), 296–302. https://doi.org/10.1016/j.neuron.2014.12.032

Montero, J. C., Seoane, S., Ocaña, A., & Pandiella, A. (2011). Inhibition of Src Family Kinases and Receptor Tyrosine Kinases by Dasatinib: Possible Combinations in Solid Tumors. *Clinical Cancer Research*, *17*(17), 5546–5552. https://doi.org/10.1158/1078-0432.CCR-10-2616

Muñoz-Espín, D., & Serrano, M. (2014). Cellular senescence: From physiology to pathology. *Nature Reviews Molecular Cell Biology*, *15*(7), 482–496. https://doi.org/10.1038/nrm3823

Musi, N., Valentine, J. M., Sickora, K. R., Baeuerle, E., Thompson, C. S., Shen, Q., & Orr, M. E. (2018). Tau protein aggregation is associated with cellular senescence in the brain. *Aging Cell*, *17*(6), e12840. https://doi.org/10.1111/acel.12840

Nambiar, A., Kellogg, D., Justice, J., Goros, M., Gelfond, J., Pascual, R., Hashmi, S., Masternak, M., Prata, L., LeBrasseur, N., Limper, A., Kritchevsky, S., Musi, N., Tchkonia, T., & Kirkland, J. (2023). Senolytics dasatinib and quercetin in idiopathic pulmonary fibrosis: Results of a phase I, single-blind, single-center, randomized, placebo-controlled pilot trial on feasibility and tolerability. *eBioMedicine*, *90*, 104481. https://doi.org/10.1016/j.ebiom.2023.104481

Navakkode, S., & Kennedy, B. K. (2024). Neural ageing and synaptic plasticity: Prioritizing brain health in healthy longevity. *Frontiers in Aging Neuroscience*, *16*, 1428244. https://doi.org/10.3389/fnagi.2024.1428244

OECD & European Union. (2022). *Health at a Glance: Europe 2022: State of Health in the EU Cycle*. OECD. https://doi.org/10.1787/507433b0-en

Ohta, T., Kikuta, K., Imamura, H., Takagi, Y., Nishimura, M., Arakawa, Y., Hashimoto, N., & Nozaki, K. (2006). Administration of *Ex vivo*-expanded Bone Marrow-derived Endothelial Progenitor Cells Attenuates Focal Cerebral Ischemia-reperfusion Injury in

Rats. *Neurosurgery*, *59*(3), 679–686. https://doi.org/10.1227/01.NEU.0000229058.08706.88

Plagg, B., & Zerbe, S. (2020). How does the environment affect human ageing? An interdisciplinary review. *Journal of Gerontology and Geriatrics*, *69*(1), 53–67. https://doi.org/10.36150/2499-6564-420

Prisco, A. R., Prisco, M. R., Carlson, B. E., & Greene, A. S. (2015). TNF-α increases endothelial progenitor cell adhesion to the endothelium by increasing bond expression and affinity. *American Journal of Physiology-Heart and Circulatory Physiology*, *308*(11), H1368–H1381. https://doi.org/10.1152/ajpheart.00496.2014

Roos, C. M., Zhang, B., Palmer, A. K., Ogrodnik, M. B., Pirtskhalava, T., Thalji, N. M., Hagler, M., Jurk, D., Smith, L. A., Casaclang-Verzosa, G., Zhu, Y., Schafer, M. J., Tchkonia, T., Kirkland, J. L., & Miller, J. D. (2016). Chronic senolytic treatment alleviates established vasomotor dysfunction in aged or atherosclerotic mice. *Aging Cell*, *15*(5), 973–977. https://doi.org/10.1111/acel.12458

Rossowska, J., Anger, N., Szczygieł, A., Mierzejewska, J., & Pajtasz-Piasecka, E. (2017). Intratumoral Lentivector-Mediated TGF-β1 Gene Downregulation As a Potent Strategy for Enhancing the Antitumor Effect of Therapy Composed of Cyclophosphamide and Dendritic Cells. *Frontiers in Immunology*, *8*, 713. https://doi.org/10.3389/fimmu.2017.00713

Rudnicka-Drożak, E., Drożak, P., Mizerski, G., & Drożak, M. (2022). Endothelial Progenitor Cells in Neurovascular Disorders—A Comprehensive Overview of the Current State of Knowledge. *Biomedicines*, *10*(10), 2616. https://doi.org/10.3390/biomedicines10102616

Salas, I. H., Burgado, J., & Allen, N. J. (2020). Glia: Victims or villains of the aging brain? *Neurobiology of Disease*, *143*, 105008. https://doi.org/10.1016/j.nbd.2020.105008

Samakkarnthai, P., Saul, D., Zhang, L., Aversa, Z., Doolittle, M. L., Sfeir, J. G., Kaur, J., Atkinson, E. J., Edwards, J. R., Russell, G. G., Pignolo, R. J., Kirkland, J. L., Tchkonia, T., Niedernhofer, L. J., Monroe, D. G., Lebrasseur, N. K., Farr, J. N., Robbins, P. D., & Khosla, S. (2023). *In vitro* and *in vivo* effects of zoledronic acid on senescence and senescence-associated secretory phenotype markers. *Aging*, *15*(9), 3331–3355. https://doi.org/10.18632/aging.204701

Shi, Q., Rafii, S., Wu, M. H.-D., Wijelath, E. S., Yu, C., Ishida, A., Fujita, Y., Kothari, S., Mohle, R., Sauvage, L. R., Moore, M. A. S., Storb, R. F., & Hammond, W. P. (1998). Evidence for Circulating Bone Marrow-Derived Endothelial Cells. *Blood*, *92*(2), 362–367. https://doi.org/10.1182/blood.V92.2.362

Shyu, W.-C., Lin, S.-Z., Chiang, M.-F., Su, C.-Y., & Li, H. (2006). Intracerebral Peripheral Blood Stem Cell ($CD34^+$) Implantation Induces Neuroplasticity by Enhancing β1 Integrin-Mediated Angiogenesis in Chronic Stroke Rats. *The Journal of Neuroscience*, *26*(13), 3444–3453. https://doi.org/10.1523/JNEUROSCI.5165-05.2006

Sobrino, T., Arias, S., Pérez-Mato, M., Agulla, J., Brea, D., Rodríguez-Yáñez, M., & Castillo, J. (2011). $Cd34^+$ progenitor cells likely are involved in the good functional recovery after intracerebral hemorrhage in humans. *Journal of Neuroscience Research*, *89*(7), 979–985. https://doi.org/10.1002/jnr.22627

Steinacker, P., Barschke, P., & Otto, M. (2019). Biomarkers for diseases with TDP-43 pathology. *Molecular and Cellular Neuroscience*, *97*, 43–59. https://doi.org/10.1016/j.mcn.2018.10.003

Sunderland, P., Alshammari, L., Ambrose, E., Torella, D., & Ellison-Hughes, G. M. (2023). Senolytics rejuvenate the reparative activity of human cardiomyocytes and endothelial cells. *The Journal of Cardiovascular Aging*. https://doi.org/10.20517/jca.2023.07

Sung, P.-H., Lin, H.-S., Lin, W.-C., Chang, C.-C., Pei, S.-N., Ma, M.-C., Chen, K.-H., Chiang, J. Y., Chang, H.-W., Lee, F.-Y., Lee, M. S., & Yip, H.-K. (2018). Intra-carotid arterial transfusion of autologous circulatory derived CD34+ cells for old ischemic stroke patients—A phase I clinical trial to evaluate safety and tolerability. *American Journal of Translational Research*, *10*(9), 2975–2989.

Sweeney, M. D., Zhao, Z., Montagne, A., Nelson, A. R., & Zlokovic, B. V. (2019). Blood-Brain Barrier: From Physiology to Disease and Back. *Physiological Reviews*, *99*(1), 21–78. https://doi.org/10.1152/physrev.00050.2017

Thinard, R., Farkas, A. E., Halasa, M., Chevalier, M., Brodaczewska, K., Majewska, A., Zdanowski, R., Paprocka, M., Rossowska, J., Duc, L. T., Greferath, R., Krizbai, I., Van Leuven, F., Kieda, C., & Nicolau, C. (2022). "Endothelial Antibody Factory" at the Blood Brain Barrier: Novel Approach to Therapy of Neurodegenerative Diseases. *Pharmaceutics*, *14*(7), 1418. https://doi.org/10.3390/pharmaceutics14071418

Tiwari, S., Atluri, V., Kaushik, A., Yndart, A., & Nair, M. (2019). Alzheimer's disease: Pathogenesis, diagnostics, and therapeutics. *International Journal of Nanomedicine, Volume 14*, 5541–5554. https://doi.org/10.2147/IJN.S200490

Tóth, R., Farkas, A. E., Krizbai, I. A., Makra, P., Bari, F., Farkas, E., & Menyhárt, Á. (2021). Astrocyte Ca2+ Waves and Subsequent Non-Synchronized Ca2+ Oscillations Coincide with Arteriole Diameter Changes in Response to Spreading Depolarization. *International Journal of Molecular Sciences*, *22*(7), 3442. https://doi.org/10.3390/ijms22073442

Wang, Y., Chang, J., Liu, X., Zhang, X., Zhang, S., Zhang, X., Zhou, D., & Zheng, G. (2016). Discovery of piperlongumine as a potential novel lead for the development of senolytic agents. *Aging*, *8*(11), 2915–2926. https://doi.org/10.18632/aging.101100

Wei, J., Blum, S., Unger, M., Jarmy, G., Lamparter, M., Geishauser, A., Vlastos, G. A., Chan, G., Fischer, K.-D., Rattat, D., Debatin, K.-M., Hatzopoulos, A. K., & Beltinger, C. (2004). Embryonic endothelial progenitor cells armed with a suicide gene target hypoxic lung metastases after intravenous delivery. *Cancer Cell*, *5*(5), 477–488. https://doi.org/10.1016/S1535-6108(04)00116-3

World population ageing 2020 Highlights: Living arrangements of older persons. (2020). United Nations.

Xin, B., Liu, C.-L., Yang, H., Peng, C., Dong, X.-H., Zhang, C., Chen, A. F., & Xie, H.-H. (2016). Prolonged Fasting Improves Endothelial Progenitor Cell-Mediated Ischemic Angiogenesis in Mice. *Cellular Physiology and Biochemistry*, *40*(3–4), 693–706. https://doi.org/10.1159/000452581

Xu, M., Pirtskhalava, T., Farr, J. N., Weigand, B. M., Palmer, A. K., Weivoda, M. M., Inman, C. L., Ogrodnik, M. B., Hachfeld, C. M., Fraser, D. G., Onken, J. L., Johnson, K. O., Verzosa, G. C., Langhi, L. G. P., Weigl, M., Giorgadze, N., LeBrasseur, N. K., Miller, J. D., Jurk, D., … Kirkland, J. L. (2018). Senolytics improve physical function and increase lifespan in old age. *Nature Medicine*, *24*(8), 1246–1256. https://doi.org/10.1038/s41591-018-0092-9

Xue, S., Shen, K., Wang, K., Ge, W., Mao, T., Li, S., Zhang, X., Xu, H., Wang, Y., Yao, J., Yue, M., Ma, J., Wang, Y., Shentu, D., Cui, J., & Wang, L. (2022). Prediction of Survival and Tumor Microenvironment Infiltration Based on Pyroptosis-Related

lncRNAs in Pancreatic Cancer. *Disease Markers*, *2022*, 1–22. https://doi.org/10.1155/2022/5634887

Yao, M., Wei, Z., Nielsen, J. S., Kakazu, A., Ouyang, Y., Li, R., Chu, T., Scafidi, S., Lu, H., Aggarwal, M., & Duan, W. (2024). *Senolytic therapy preserves blood-brain barrier integrity and promotes microglia homeostasis in a tauopathy model*. Neuroscience. https://doi.org/10.1101/2024.03.25.586662

Yuan, X., Mei, B., Zhang, L., Zhang, C., Zheng, M., Liang, H., Wang, W., Zheng, J., Ding, L., & Zheng, K. (2016). Enhanced penetration of exogenous EPCs into brains of APP/PS1 transgenic mice. *American Journal of Translational Research*, *8*(3), 1460–1470.

Zhang, P., Kishimoto, Y., Grammatikakis, I., Gottimukkala, K., Cutler, R. G., Zhang, S., Abdelmohsen, K., Bohr, V. A., Misra Sen, J., Gorospe, M., & Mattson, M. P. (2019). Senolytic therapy alleviates Aβ-associated oligodendrocyte progenitor cell senescence and cognitive deficits in an Alzheimer's disease model. *Nature Neuroscience*, *22*(5), 719–728. https://doi.org/10.1038/s41593-019-0372-9

Zhang, S., Zhi, Y., Li, F., Huang, S., Gao, H., Han, Z., Ge, X., Li, D., Chen, F., Kong, X., & Lei, P. (2018). Transplantation of *in vitro* cultured endothelial progenitor cells repairs the blood-brain barrier and improves cognitive function of APP/PS1 transgenic AD mice. *Journal of the Neurological Sciences*, *387*, 6–15. https://doi.org/10.1016/j.jns.2018.01.019

Zhang, Y., Herbert, B., Rajashekhar, G., Ingram, D. A., Yoder, M. C., Clauss, M., & Rehman, J. (2009). Premature senescence of highly proliferative endothelial progenitor cells is induced by tumor necrosis factor-α *via* the p38 mitogen-activated protein kinase pathway. *The FASEB Journal*, *23*(5), 1358–1365. https://doi.org/10.1096/fj.08-110296

Zhang, Z. G., Zhang, L., Jiang, Q., & Chopp, M. (2002). Bone Marrow-Derived Endothelial Progenitor Cells Participate in Cerebral Neovascularization After Focal Cerebral Ischemia in the Adult Mouse. *Circulation Research*, *90*(3), 284–288. https://doi.org/10.1161/hh0302.104460

Zhu, Y., Doornebal, E. J., Pirtskhalava, T., Giorgadze, N., Wentworth, M., Fuhrmann-Stroissnigg, H., Niedernhofer, L. J., Robbins, P. D., Tchkonia, T., & Kirkland, J. L. (2017). New agents that target senescent cells: The flavone, fisetin, and the BCL-XL inhibitors, A1331852 and A1155463. *Aging*, *9*(3), 955–963. https://doi.org/10.18632/aging.101202

Zhu, Y., Tchkonia, T., Fuhrmann-Stroissnigg, H., Dai, H. M., Ling, Y. Y., Stout, M. B., Pirtskhalava, T., Giorgadze, N., Johnson, K. O., Giles, C. B., Wren, J. D., Niedernhofer, L. J., Robbins, P. D., & Kirkland, J. L. (2016). Identification of a novel senolytic agent, navitoclax, targeting the Bcl-2 family of anti-apoptotic factors. *Aging Cell*, *15*(3), 428–435. https://doi.org/10.1111/acel.12445

Zhu, Y., Tchkonia, T., Pirtskhalava, T., Gower, A. C., Ding, H., Giorgadze, N., Palmer, A. K., Ikeno, Y., Hubbard, G. B., Lenburg, M., O'Hara, S. P., LaRusso, N. F., Miller, J. D., Roos, C. M., Verzosa, G. C., LeBrasseur, N. K., Wren, J. D., Farr, J. N., Khosla, S., … Kirkland, J. L. (2015). The Achilles' heel of senescent cells: From transcriptome to senolytic drugs. *Aging Cell*, *14*(4), 644–658. https://doi.org/10.1111/acel.12344

Zuchero, Y. J. Y., Chen, X., Bien-Ly, N., Bumbaca, D., Tong, R. K., Gao, X., Zhang, S., Hoyte, K., Luk, W., Huntley, M. A., Phu, L., Tan, C., Kallop, D., Weimer, R. M., Lu, Y., Kirkpatrick, D. S., Ernst, J. A., Chih, B., Dennis, M. S., & Watts, R. J. (2016). Discovery of Novel Blood-Brain Barrier Targets to Enhance Brain Uptake of Therapeutic Antibodies. *Neuron*, *89*(1), 70–82. https://doi.org/10.1016/j.neuron.2015.11.024